Quantum Hydrodynamics and the SYK Model at Next-to-Leading Order

by

Wyatt Reeves

BSc with Honors in Mathematical Physics, University of Alberta, 2017

A THESIS SUBMITTED IN PARTIAL FULFILLMENT
OF THE REQUIREMENTS FOR THE DEGREE OF

Master of Science

in

THE FACULTY OF GRADUATE AND POSTDOCTORAL STUDIES
(Physics)

The University of British Columbia
(Vancouver)

April 2019

The following individuals certify that they have read, and recommend to the Faculty of Graduate and Postdoctoral Studies for acceptance, the thesis entitled:

Quantum Hydrodynamics and the SYK Model at Next-to-Leading Order

submitted by **Wyatt Reeves** in partial fulfillment of the requirements for the degree of **Master of Science** in **Physics**.

Examining Committee:

Moshe Rozali, Physics
Supervisor

Mark van Raamsdonk, Physics
Examining Committee Member

Abstract

There has been renewed interest in understanding the details and origins of chaos in quantum systems with many degrees of freedom. Chaos plays a significant role in holographic theories, hydrodynamic transport, and even the strange metal phase of condensed matter systems. With this importance, discovering a unified origin that yields universal results for chaotic systems is clearly desirable.

In this thesis, we investigate the conjectured hydrodynamic origin of quantum many-body chaos, first posited in [1], by testing it with the next-to-leading order Sachdev-Ye-Kitaev (SYK) model. We provide a review of how hydrodynamic theories are constructed, and how hydrodynamic theories with a certain symmetry possess all the standard features of chaos. We then review the leading order SYK model, demonstrate its chaotic behaviour, and compare it with the predictions of the hydrodynamic theory. We finally perform an in-depth investigation of the next-to-leading order SYK model, demonstrating that, while one sector of the theory satisfies the conjecture, another sector does not admit a hydrodynamic description. This shows that the conjecture must be modified to account for near-maximally chaotic theories.

Lay Summary

Chaos, or the butterfly effect, refers to the phenomenon by which small perturbations in a physical system cause changes that grow exponentially with time. While best known for its manifestations in weather and other classical systems, chaotic behaviour can be observed on microscopic scales, where quantum mechanical effects become relevant. Understanding such quantum chaotic systems is important for understanding the properties of fluids, superconductors, and even black holes. In this thesis, we make further steps towards understanding why certain quantum mechanical systems are chaotic, by investigating a proposal for the origin of chaos.

Preface

This dissertation is original, unpublished, independent work by the author, W. Reeves, with supervision by M. Rozali. Chapters 2 and 3 consist primarily of review of relevant material, while chapters 4 and 5 are primarily original work.

Table of Contents

List of Tables

List of Figures

List of Abbreviations

ADS Anti-de Sitter

CFT Conformal Field Theory

CTP Closed Time Path

EFT Effective Field theory

NLO Next-to-Leading Order

OTOC Out-of-Time-Ordered Correlator

SYK Sachdev-Ye-Kitaev

TOC Time-Ordered Correlator

Acknowledgments

I would like to thank Moshe Rozali for providing me with this project and his supervision. I would like to thank Sean Cooper, Alex May, Dominik Neuenfeld, Chris Waddell, David Wakeham, and Jordan Wilson-Gerow for several helpful conversations.

Dedication

To my parents, for their love and support.

Chapter 1

Introduction

Quantum many-body chaos lacks a universal description despite the ubiquity of chaos in thermal systems. The use of Out-of-Time-Ordered Correlators (OTOCs) of operators consisting of a few degrees of freedom,

$$C(t) = \langle V(t)W(0)V(t)W(0)\rangle, \tag{1.1}$$

to diagnose chaos has been well documented since its proposal [2]. In theories with a large parameter N (e.g., the number of particles) the OTOC is small at early times, $C(t) \sim O(N^{-1})$, until the characteristic relaxation time t_r when all two-point functions have died off. The typical signifier of chaos is exponential growth in the OTOC after the relaxation time:

$$C(t) \sim \frac{1}{N} e^{\lambda t}, t_r \ll t \ll t_s, \tag{1.2}$$

where λ is the Lyapunov exponent, and $t_s = \frac{1}{\lambda}\log N$ is the scrambling time when the OTOC becomes $O(1)$. If the operators are also separated by large distances, then this exponential behaviour often becomes $C(t,x) \sim \frac{1}{N} e^{\lambda(t-\frac{|x|}{v_B})}$, where v_B is the butterfly velocity. Other forms of spatial dependence such as diffusive spreading can also arise, $C(t,x) \sim \frac{1}{N} e^{(\lambda t - \frac{|x|^2}{D_0 t})}$. This exponential growth in time has been coined "scrambling", and indicates the growth in the number of degrees of freedom affected by V after perturbing the system with W.

It was shown in [3] that such growth is bounded: $\lambda \leq 2\pi/\beta$. This bound is saturated for theories which have a holographic dual description of an Anti-de Sitter (ADS) black hole, where the OTOC can be viewed as a scattering amplitude near the black hole horizon [4, 5]. Thus, saturation of the chaos bound in a many-body quantum theory is a key indicator that the theory is holographic. Unfortunately, determining the behaviour for such OTOCs often requires complicated, model-specific calculations [6, 7]. This is partially a result of the lack of a general description for the origin of scrambling and chaos.

Blake, Lee, and Liu [1] have proposed that the origin of chaos lies in quantum hydrodynamics. They conjecture that chaos arises due to a "shift symmetry" in the hydrodynamic effective action, leading to a buildup of a "hydrodynamic cloud" that serves as the mechanism which scrambles operators among many degrees of freedom. This symmetry yields an exponentially growing fluid mode, and leads to a variety of results such as exponential growth in the OTOCs of generic operators, the lack of such growth in Time-Ordered Correlators (TOCS), and an interesting "pole-skipping" phenomenon in the energy two-point function. This pole-skipping in particular is very useful, as it provides a straightforward way to calculate both the Lyapunov exponent and butterfly velocity. This conjecture has been verified for both the Sachdev-Ye-Kitaev (SYK) [6] and SYK chain models [8], chaotic Conformal Field Theorys (CFTS) [9], Einstein gravity [10], and higher-derivative gravity theories [11].

In all of these models, the conjecture was checked at leading order in perturbation theory (e.g., at leading order in the inverse coupling for the SYK model), where each model is maximally chaotic. However, at Next-to-Leading Order (NLO), negative corrections to the Lyapunov exponent have been shown to arise in many of these models, most notably from stringy effects in ADS black holes [5] and from the massive modes in the SYK model [6], making these theories only near-maximally chaotic.

In this thesis, we will investigate the SYK model at NLO, comparing SYK model-specific calculations to general predictions from hydrodynamics. We first introduce hydrodynamics and the conjectured origin of chaos in Chapter 2, followed by the SYK model at leading order in Chapter 3. We then determine how hydrodynamical pole-skipping is modified in $0 + 1$ dimensional theories, comparing the predictions to the leading order SYK energy two-point function in Chapter 4. We will then

discuss the NLO correction to the soft mode theory in Chapter 5, demonstrating that the model remains maximally chaotic at NLO, retains the shift symmetry (in this case a full $\mathrm{SL}(2,\mathbb{R})$ symmetry), and possesses the $0+1$ dimensional version of pole-skipping. Finally, we will discuss the massive modes, their role in reducing the Lyapunov exponent, and their impact on the conjectured hydrodynamic origin of chaos.

Chapter 2

Hydrodynamics

In this chapter, we review the hydrodynamic effective theory and its relation to chaotic theories, closely following [1].

2.1 Preliminaries

Quantum hydrodynamics is a universal sector of all quantum many-body systems. It is the low energy Effective Field theory (EFT) for gapless modes associated with conserved quantities, such as energy and momentum. We follow the theory as laid out in [1, 12], formulating it for systems where the only conserved quantity is energy.

We describe the theory using what is essentially the Lagrange description of fluids; we define fluid spacetime coordinates $\sigma^A = (\sigma^0, \sigma^i)$, where the σ^i labels each fluid element via its position in the fluid spacetime, and σ^0 is interpreted as the "internal clock" for each fluid element. The hydrodynamic degrees of freedom are given by mappings from the fluid spacetime to two copies of physical spacetime on the legs of a Closed Time Path (CTP) contour, $X^\mu_s(\sigma), s = 1, 2$. The need for a CTP (also known as a Schwinger-Keldysh contour) is familiar from the study of non-equilibrium systems (see Appendix A for details regarding the Schwinger-Keldysh formalism). Additionally, a local inverse temperature for each fluid element is given, $\beta(\sigma^A)$. The system begins in some initial state ρ_0, often a thermal state, and its evolution is governed by the Schwinger-Keldysh path integral with an effective

hydrodynamic action I_{hydro}.

To justify the above description and find the correct form of the action, we follow the standard story of EFTs: identify the correct symmetries, write down the most general action that satisfies them, and find the correct physical interpretation of the degrees of freedom. To find the relevant symmetries, consider a theory with a single conserved current J_μ and its generating functional, with sources $A_{s\mu}$ on each leg of the CTP:

$$e^{W[A_{1\mu},A_{2\mu}]} = \text{Tr}\left(\rho_0 \mathcal{T}_C e^{i\int A_{1\mu}J_1^\mu - A_{2\mu}J_2^\mu}\right). \tag{2.1}$$

Because J^μ is conserved, the generating functional is invariant under gauge transformations $A_{s\mu} \to A_{s\mu} + \partial_\mu \lambda_s$ for any function λ_s. We can then find a generating functional written as a path integral over a local action S by promoting the symmetry parameters λ_s to physical degrees of freedom:

$$e^{W[A_{1\mu},A_{2\mu}]} = \int D\varphi_1 D\varphi_2 e^{iS[B_{1\mu},B_{2\mu}]},\ B_{s\mu} \coloneqq A_{s\mu} + \partial_\mu \varphi_s. \tag{2.2}$$

The generating functional defined this way is manifestly invariant under gauge transformations, and we have a local action that yields a generating functional for our conserved current.

If our conserved current is the stress-energy tensor, we know that turning on sources corresponds to putting the system in a curved spacetime with metric $g_{s\mu\nu}$ on each leg of the CTP. Conservation of the stress-energy tensor then leads to the gauge symmetry being identified as diffeomorphism invariance of the metric,

$$g_{s\mu\nu}(x_s) \to g_{s\rho\sigma}(y_s(x_s))\frac{\partial y_s^\rho}{\partial x_s^\mu}\frac{\partial y_s^\sigma}{\partial x_s^\nu}.$$

Promoting the symmetry parameters to degrees of freedom means our hydrodynamic action is given by

$$\begin{aligned} e^{W[g_1,g_2]} &= \int DX_1 DX_2 D\beta\ e^{iI_{\text{hydro}}[h_1,h_2,\beta]}, \\ h_{sAB} &= g_{s\mu\nu}(X_s)\frac{\partial X_s^\mu}{\partial \sigma^A}\frac{\partial X_s^\nu}{\partial \sigma^B}, \end{aligned} \tag{2.3}$$

where we have also introduced a local temperature $\beta(\sigma)$. Interpreting the σ^A as coordinates on the fluid spacetime, and X_s as the coordinates on the physical spacetime, we've found the general form of our action and justified the description given at the start of the section. This is an EFT for a system whose only conserved current is the stress-energy tensor, described with the associated long-lived gapless degrees of freedom.

There are a few additional symmetries to impose. The action should not depend on how we initially choose to label the fluid elements in the fluid spacetime, nor on how each fluid element tracks time. We thus demand the action I_{hydro} be invariant under diffeomorphisms of the spatial or time components of σ^A, but not both:

$$\begin{aligned} \sigma^0 \to \sigma^0, \quad \sigma^i \to \sigma'^i(\sigma^i), \\ \sigma^0 \to \sigma'^0(\sigma^0, \sigma^i), \quad \sigma^i \to \sigma^i. \end{aligned} \tag{2.4}$$

This is weaker than general diffeomorphism invariance by necessity: allowing, for example, $\sigma^i \to \sigma'^i(\sigma^0, \sigma^i)$ would mean that the fluid element σ^i changes with time, thus treating actual fluid motion as relabeling.

We also require that the action satisfies the unitarity conditions

$$I^*_{\text{hydro}}[h_1, h_2, \beta] = -I_{\text{hydro}}[h_2, h_1, \beta], \tag{2.5}$$

$$I_{\text{hydro}}[h_1 = h_2, \beta] = 0, \tag{2.6}$$

$$\text{Im} I_{\text{hydro}} \geq 0. \tag{2.7}$$

The first condition is from CPT invariance of the Schwinger-Keldysh path integral, the second from unitarity of time evolution (since setting $h_1 = h_2$ amounts to evolving forward and backward in time in the exact same way), and the third from requiring that the path integral be well defined (since a negative imaginary part of the action would lead to exponential growth in the path integral).

Finally, we require the action to be invariant under what is referred to in [12] as "a Z_2 dynamical KMS symmetry". This symmetry takes a simple form by using time diffeomorphism to fix the local temperature,

$$\beta(\sigma^A) = \beta = \beta_0 \frac{1}{2}(\sqrt{-h_{100}} + \sqrt{-h_{200}}), \tag{2.8}$$

where β_0 is some reference scale (e.g., the background inverse-temperature if we are in a thermal state). With this, the metric transforms under this symmetry as

$$\widetilde{h}_1(-\sigma,-x^i) = h_1(\sigma+i\theta,x^i),\ \widetilde{h}_2(-\sigma,-x^i) = h_2(\sigma-i(\beta_0-\theta),x^i),\ \theta\in[0,\beta_0], \quad (2.9)$$

and the action is invariant under this symmetry, $I_{\text{hydro}}[h_1,h_2,\beta] = I_{\text{hydro}}[\widetilde{h}_1,\widetilde{h}_2,\beta]$. This imposes local equilibrium and microscopic time reversal symmetry.

2.2 Lagrangian and Shift Symmetry

For our purposes, we can consider the action without external sources for a system with only energy conservation, as in [1]. We use spatial diffeomorphism invariance to set $\sigma^i = X^i_r =: x^i$, leaving $X^0_{1,2}(\sigma^0,x^i)$ as the remaining dynamical variables (recall we used time diffeomorphism invariance to fix β). We then identify $X_r = \frac{1}{2}(X^0_1 + X^0_2)$ as physical motion and $X_a = X^0_1 - X^0_2$ as quantum-statistical noises[1], and invert $X_r(\sigma^0,x_i) \equiv t$ to express the theory in terms of $\sigma(t,x^i) \coloneqq \sigma^0(t,x^i)$ and $X_a(t,x^i) \coloneqq X_a(\sigma,x^i)$. This has the additional benefit that we now have $\beta = \beta_0/\partial_t\sigma$.

We can then write down the action to quadratic order in the noise field X_a using standard EFT techniques:

$$\mathcal{L}_{\text{hydro}} = -H\partial_t X_a - G_i\partial_i X_a + \frac{i}{2}\partial_t X_a M_1 \partial_t X_a + \frac{i}{2}\partial_i X_a M_2 \partial_i X_a + O(a^3), \quad (2.10)$$

where H and G_i are functions of $\beta = \beta_0/\partial_t\sigma$ and its derivatives, and $M_{1,2}$ are differential operators constructed out of ∂_t, ∂_i, and β. The equilibrium configuration $\sigma = t, X_a = 0$ is always a solution to this Lagrangian.

We now expand around equilibrium:

$$\sigma = t + \epsilon_r(t,x^i),\ X_a = -\epsilon_a(t,x^i),\ \beta = \beta_0 + \delta\beta,\ \delta\beta = \beta_0(1-\partial_t\epsilon_r), \quad (2.11)$$

[1]This is the standard "average-difference" basis found in Schwinger-Keldysh theory. This basis generally admits the interpretation of physical motion and noise [13]. We will use this basis regularly throughout this thesis.

and expand Equation 2.10 to quadratic order in ϵ_a:

$$\mathcal{L}_{\text{hydro}} = \epsilon_a K \epsilon_r - \frac{i}{2}\epsilon_a M \epsilon_a, \quad K = \beta_0(f_1\partial_t + h_1\partial_i^2)\partial_t, \quad M = \left(M_1\partial_t + M_2\partial_i^2\right)|_{\beta=\beta_0}, \tag{2.12}$$

where we have written H and G_i as $H = f_1\delta\beta$, $G_i = h_1\partial_i\delta\beta$, where $f_1(\partial_t, \partial_i)$ and $h_1(\partial_t, \partial_i)$ are differential operators. All β dependence in $M_{1,2}$ has been set to β_0. The equation of motion for this Lagrangian is

$$(f_1\partial_t + h_1\partial_i^2)\partial_t\epsilon_r = 0, \quad \epsilon_a = 0. \tag{2.13}$$

Everything thus far has been for general theories where the only conserved quantity is energy, and the only long-lived gapless modes are those associated with energy conservation. We now demonstrate how certain hydrodynamic EFTs can predict chaotic behaviour: the key is demanding that Equation 2.12 be invariant under the "shift symmetry",

$$u(t, x^i) \to u(t, x^i) + f(t, x^i),\ u = e^{-\lambda\sigma},\ \partial_t f = \kappa(\partial_i)f, \tag{2.14}$$

where f is some function satisfying the above differential equation, λ is a constant, and $\kappa(\partial_i)$ is a differential operator with at least one derivative (or equal to zero), such that $f(t, x^i) = c$ is always a solution. Under this symmetry, we find an exponentially growing solution to Equation 2.13:

$$\epsilon = -\frac{f}{\lambda}e^{\lambda t},\ \partial_t\epsilon = \tilde{\lambda}(\partial_i)\epsilon,\ \tilde{\lambda}(\partial_i) = \lambda + \kappa(\partial_i). \tag{2.15}$$

This exponentially growing mode is responsible for the exponential growth found in OTOCs, while the symmetry protects TOCs from this exponential growth (as expected for systems without instabilities). Both the SYK and SYK chain models satisfy this symmetry; for the SYK model, with no spatial dependence, the symmetry is just a constant shift in $u(t)$, while for the SYK chain the shift is an arbitrary time-independent shift $u(t, x^i) \to u(t, x^i) + a(x^i)$, both corresponding to $\kappa = 0$.

2.3 Shift Symmetry Results

We now review the results demonstrating the chaotic behaviour of a shift symmetric theory. We investigate the behaviour of the retarded two-point functions for both the hydrodynamic mode and energy density, along with the behaviour of OTOCs and TOCs of generic few-body operators. These results will establish that any hydrodynamic theory with a shift symmetry is chaotic, and predict a phenomenon in the retarded energy two-point function called pole-skipping.

First, note that this symmetry implies that the operators f_1, h_1 have the form

$$f_1 = (\partial_t - \tilde{\lambda}(\partial_i^2))a(\partial_t, \partial_i^2),\ h_1 = (\partial_t - \tilde{\lambda}(\partial_i^2))b(\partial_t, \partial_i^2), \tag{2.16}$$

where $a(\partial_t, \partial_i), b(\partial_t, \partial_i)$ are new differential operators. This ensures that Equation 2.12 satisfies the shift symmetry.

We now need the retarded two-point function for the hydrodynamic modes,

$$G_R(x) = i\langle \epsilon_r(x)\epsilon_a(0)\rangle; \tag{2.17}$$

see Appendix A for the origin of this expression. Since Equation 2.12 is quadratic, with the term $\epsilon_a K \epsilon_r$, we can find the retarded two-point function by inverting the $K = \beta_0(f_1\partial_t + h_1\partial_i^2)\partial_t$ operator, subject to retarded boundary conditions. This is accomplished by taking the inverse Fourier transform of $G_R(\omega, k) = -1/K(\omega, k)$ with an open contour C that goes above all its poles:

$$G_R(x) = -\int_C \frac{d^d k}{(2\pi)^d} \frac{e^{-i\omega t + ik_i x^i}}{K(\omega)}. \tag{2.18}$$

Using Equation 2.12 and Equation 2.16 we can express $G_R(\omega, k)$ as

$$G_R(\omega, k) = -\frac{1}{i\beta_0\omega^2 a(\omega, k)(\omega - i\tilde{\lambda}(k))(\omega + i\mathcal{D}(\omega, k)k^2)},\ \ \mathcal{D}(\omega, k) := -\frac{b(\omega, k)}{a(\omega, k)}, \tag{2.19}$$

where we have introduced the "diffusion operator" $\mathcal{D}(\omega, k)$. The choice of contour means that when $t < 0$, we can close the contour in the upper half plane without picking up any poles, yielding zero. We will assume that the only poles in the complex ω upper half plane come from the $\omega - i\tilde{\lambda}(k)$ term. There is a line of poles

in the lower half plane from

$$\omega + i\mathcal{D}(\omega, k)k^2 = 0. \tag{2.20}$$

In the limit of small ω, k, these yield the standard energy diffusion poles $\omega = -iD_E k^2, D_E \coloneqq \mathcal{D}(0,0)$ (hence the name diffusion operator).

For a $0+1$ dimensional system (such as the SYK model), obtained by suppressing all spatial dependence, we have

$$\begin{aligned} G_R(\omega) &= -\frac{1}{i\beta_0\omega^2 a(\omega)(\omega - i\lambda)}, \\ G_R(t) &= -\theta(t)\frac{1}{\beta_0 a(i\lambda)\lambda^2}e^{\lambda t} + \cdots, \end{aligned} \tag{2.21}$$

where we have only kept the exponentially growing term. For systems with spatial dependence, we get a similar result using Equation 2.19: we perform the ω integration, and look at the exponentially growing term from the pole at

$$\omega - i\tilde{\lambda}(k) = 0 \tag{2.22}$$

We see that if there is a solution to the equation

$$\tilde{\lambda}(k) + k^2\mathcal{D}(i\tilde{\lambda}, k) = 0 \tag{2.23}$$

for some $k^2 = -k_C^2 < 0$, then we obtain

$$G_R(x) = c\theta(t)e^{\overline{\lambda}(t - \frac{|x|}{v_B})}, \tag{2.24}$$

$$\overline{\lambda} \coloneqq \tilde{\lambda}(-k_C^2),\ \overline{\lambda} - k_C^2\mathcal{D}(i\overline{\lambda}, -k_c^2) = 0,\ v_B \coloneqq \frac{\overline{\lambda}}{k_C}. \tag{2.25}$$

Thus we see that assuming shift symmetry gives us the expected behaviour for the retarded two-point function in a chaotic system.

Using these correlators with the expressions for the energy density found in [1], Appendix A, we can also find the retarded energy density two-point function

$$G_R^{\mathcal{E}\mathcal{E}}(x) = i\langle \mathcal{E}_r(x)\mathcal{E}_a(0)\rangle \tag{2.26}$$

to be

$$G_R^{\mathcal{E}\mathcal{E}} = \beta_0 \frac{(\omega - i\tilde{\lambda}(k))k^2 b(w,k)}{\omega + i\mathcal{D}(\omega,k)k^2}. \tag{2.27}$$

We see the same line of diffusion poles from Equation 2.20, $\omega + i\mathcal{D}(\omega, k^2) = 0$. Crucially, we see that this line of poles coincides with the zero from the $\omega - i\tilde{\lambda}(k)$ factor in the numerator precisely when ω and k obtain the same values that yielded the Lyapunov exponent and butterfly velocity in Equation 2.25. This phenomenon of "pole-skipping" implies that calculating the retarded energy two-point function and determining its singular behaviour allows one to simply read off the Lyapunov exponent and butterfly velocity. Things must be modified slightly for theories with no spatial dependence, which will be discussed in Section 4.2.

The final important result is regarding OTOCs and TOCs. Without going into too much detail, we split any operator involving only a few degrees of freedom $V(t)$ into a "bare operator" $\widehat{V}$ that doesn't communicate with any other bare operator, along with the bare operator dressed by a "hydrodynamic cloud":

$$V(t) = \widehat{V}(t) + L_t^{(1)}[\widehat{V}\varepsilon](t) + \cdots, \ \langle \widehat{V}\widehat{W}\rangle = 0, \tag{2.28}$$

where $L_t^{(1)}$ is a differential operator that couples the bare operator with the hydrodynamic mode.

Generically, OTOCs require a "doubly folded" time-path that goes forward and back twice, as in Figure 2.1, not once like with a CTP. Given this path, any four-point function between any four operators A, B, C, D can be given by

$$\langle T_C A_{i_1}(t_1) B_{i_2}(t_2) C_{i_3}(t_3) D_{i_4}(t_4)\rangle, \tag{2.29}$$

where $i_k = 1, 2, 3, 4$ tells us which leg of the path the operator is inserted on. For example, to get the OTOC in Equation 1.1, we can use

$$\langle T_C V_1(t_1) V_2(t_2) W_1(t_3) W_3(t_4)\rangle, \tag{2.30}$$

where $t_{1,2} \approx 0$ and $t_{3,4} \approx t, t_r \gg t \gg t_s$. Note that we can also obtain a more

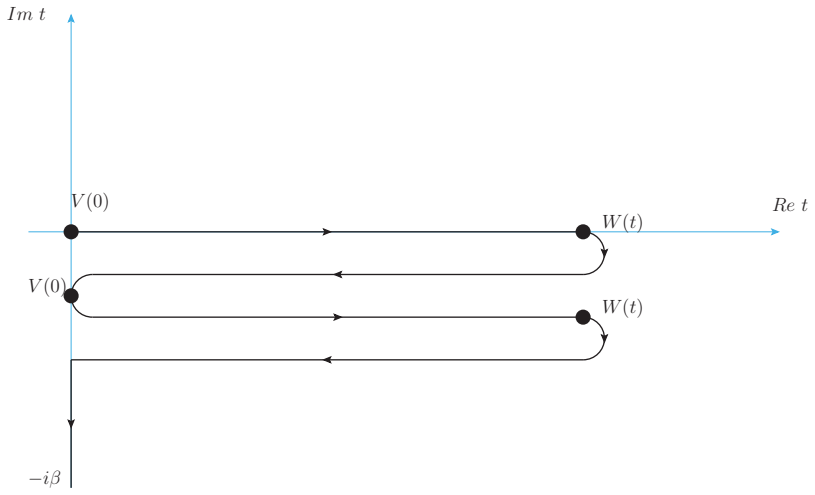

Figure 2.1: A diagram of an out-of-time-ordered correlator. The placement of the operators along the doubly-folded contour ensures the proper ordering of the operators.

standard TOC, e.g., (with $t_1 < t_2 < t_3 < t_4$),

$$\langle T_C V_1(t_1) V_2(t_2) W_3(t_3) W_4(t_4) \rangle. \tag{2.31}$$

Note that there are many other orderings of operators one could use for a TOC; for example, [1] often uses the ordering $\langle V(0)W(t)W(t)V(0)\rangle$, corresponding to the expectation value of the operator $W(t)W(t)$ in the state $V(0)|0\rangle$. What unites them is that the second fold in the contour can actually be made redundant; for example, one could put each of the operators in Equation 2.31 on the same leg and get the same result.

Even with the OTOC, we can actually avoid using this doubly-folded time path, thanks to the fact that, at quadratic order in ϵ, any four-point function of operators V, W reduces to various two-point functions of ϵ. Two-point functions of operators on any contour (with any number of folds) can always be reduced to two-point functions on a single CTP, due to the unitarity of time evolution. Thus, we are free to use the standard Schwinger-Keldysh formalism we have been using so far.

By assuming that the coupling respects both the shift symmetry and a "time

reversed" shift symmetry,

$$L^{(1)}_{t_1}[\langle \hat{V}(t_1)\hat{V}(t_2)\rangle e^{\pm\lambda t_1}] + L^{(1)}_{t_2}[\langle \hat{V}(t_1)\hat{V}(t_2)\rangle e^{\pm\lambda t_2}] = 0, \tag{2.32}$$

one can show that the TOC between operators V and W does not contain an exponentially growing part, while the OTOC does.

In conclusion, we have the observation that a hydrodynamic theory with a shift symmetry is chaotic, and does not contain instabilities in TOCS; the conjecture is that this is the origin of chaos (at least for a certain class of theories). An important corollary to this conjecture is that pole-skipping in the energy two-point function occurs whenever a large N theory is chaotic, making pole-skipping a necessary condition for chaos, and can be used to determine the Lyapunov exponent and butterfly velocity.

This conjecture appears to hold for a number of maximally chaotic theories, particularly the SYK models at leading order mentioned above and Einstein gravity [10]. However, the status of non-maximally chaotic theories and their relation to this conjecture is yet to be determined. The SYK model at NLO is an example of a "near-maximally" chaotic theory; the Lyapunov exponent receives a small negative correction proportional to the perturbation parameter, $\lambda = \frac{2\pi}{\beta} - \delta\lambda$. It is this theory we will be investigating to gain insight on whether near-maximal chaos is hydrodynamic in origin, or whether there is another sector to chaotic theories that must be found.

Chapter 3

SYK Model-Leading Order

In this chapter, we provide a quick overview of the SYK model and its description at leading order. Much of this section utilizes results from Section 3.3 and Section 4 in [6].

3.1 Preliminaries

The SYK model [14, 15] has received a great deal of focus since its proposal, thanks to the wealth of phenomena it exhibits, along with its computational simplicity. The model describes N Majorana fermions with all-to-all interactions, with couplings sampled from independent random Gaussian distributions with zero mean and the same variance:

$$\begin{aligned} H &= \frac{i^{q/2}}{q!} \sum_{j_1, j_2 \cdots j_q} j_{j_1, j_2 \cdots j_q} \psi_{j_1} \psi_{j_2} \cdots \psi_{j_q}, \\ \langle j^2_{j_1, j_2 \cdots j_q} \rangle_J &= \frac{J^2 (q-1)!}{N^{q-1}} = \frac{2^{q-1} \mathcal{J}^2 (q-1)!}{q N^{q-1}}, \quad \{\psi_i, \psi_j\} = 2\delta_{ij}. \end{aligned} \tag{3.1}$$

ψ_i are the Majorana operators, which are effectively N dimensional Dirac matrices. The variance of the random couplings $j_{\ldots}$ defines the effective one dimensional coupling J, and its scaling with N is chosen to give an interesting large N limit, while the $(q-1)!$ term simplifies some expressions. The second formula defines a rescaled coupling $\mathcal{J}$ that is useful for some formula (e.g., in [6]). We study the

model in the regime $N \gg \beta J \gg 1$, allowing us to consider only leading order effects in N, while working up to NLO in the inverse dimensionless coupling $1/\beta J$.

We will be working in Euclidean time $\tau = it$ at finite temperature. For any particular sampling of couplings $j_{\ldots}$, the path integral is

$$Z(\beta) = \int \mathcal{D}\psi \exp\left[-\int d\tau \left(\frac{1}{2}\sum_i \psi_i \partial_\tau \psi_i + \sum_{j_1, j_2 \cdots j_q} j_{j_1, j_2 \cdots j_q} \psi_{j_1} \psi_{j_2} \cdots \psi_{j_q}\right)\right]. \tag{3.2}$$

It turns out that taking the disorder average over the random couplings gives a simple, classical result. We introduce a bilocal field $\widetilde{G}(\tau_1, \tau_2)$ and Lagrange multiplier field $\widetilde{\Sigma}(\tau_1, \tau_2)$ that sets $\widetilde{G}$ equal to the averaged two-point function $\frac{1}{N}\sum_j \psi_j(\tau_1)\psi_j(\tau_2)$. We can then perform the integral over ψ:

$$\begin{aligned} \langle Z(\beta)\rangle_J &= \int \mathcal{D}\widetilde{G}\mathcal{D}\widetilde{\Sigma}\ \exp\left(-N\, I[\widetilde{G}, \widetilde{\Sigma}]\right), \\ I[G, \Sigma] &= -\log \mathrm{Pf}(\partial_t - \Sigma) + \frac{1}{2}\int d\tau_1 d\tau_2 \left[\Sigma G - \frac{J^2}{q} G^q\right]. \end{aligned} \tag{3.3}$$

The factor of N multiplying the whole action I means that taking the large N limit is a classical limit (similar to taking $\hbar \to 0$). The classical equations of motion are then found from finding the saddle point, and one can show that the equations are the same as the Schwinger-Dyson equations for the two-point function G and self-energy Σ,

$$G(\tau) = (\partial_\tau - \Sigma(\tau))^{-1}\,,\ \Sigma(\tau) = J^2 G(\tau)^{q-1}. \tag{3.4}$$

The first equation can be seen as the standard relationship between the full two-point function $G(\tau)$, the free propagator ∂_τ^{-1}, and the self-energy $\Sigma(\tau)$. This is shown diagrammatically in Figure 3.1.

In the limit of strong coupling (or equivalently, long time), we can neglect the ∂_τ term; the resulting action and SD equations are invariant under arbitrary reparameterizations of time $f(\tau)$,

$$\begin{aligned} G(\tau_1, \tau_2) &\to G(f(\tau_1), f(\tau_2))|f'(\tau_1)|^{\Delta}|f'(\tau_2)|^{\Delta}, \\ \Sigma(\tau_1, \tau_2) &\to \Sigma(f(\tau_1), f(\tau_2))|f'(\tau_1)|^{1-\Delta}|f'(\tau_2)|^{1-\Delta}. \end{aligned} \tag{3.5}$$

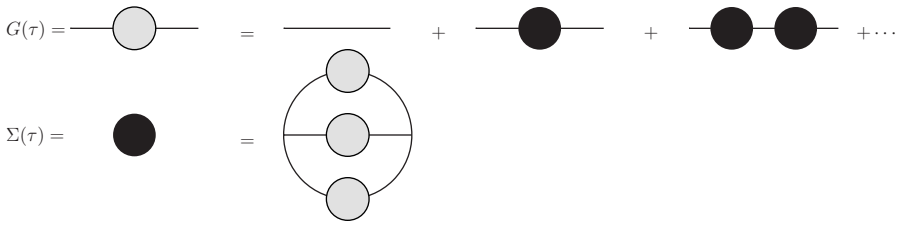

Figure 3.1: A diagrammatic representation of the Schwinger-Dyson equations. The first line is the standard representation of the two-point function in terms of the self-energy, while the second line expresses the self energy in terms of the two point function.

where $\Delta = 1/q$ is the conformal weight of the Green's function. The limit where we neglect the ∂_τ term is thus named the conformal limit.

For example, starting with the zero temperature solution

$$G_{\beta=\infty}(\tau_1, \tau_2) = -b^{\Delta}|J(\tau_1 - \tau_2)|^{-2\Delta}\text{sgn}(\tau_1 - \tau_2), \tag{3.6}$$

we can obtain the set of all solutions at a given inverse-temperature β by applying Equation 3.5 with $f(\tau) = e^{\frac{2\pi i}{\beta} g(\tau)}$, where g is a diffeomorphism. This is similar to the way finite temperature two-dimensional CFTs are obtained by exponentiating the zero temperature theory [16]. Every individual solution is unchanged by the transformation $f \to \frac{af+b}{cf+d}, a, b, c, d \in \mathbb{R}$; the reparameterization symmetry has been spontaneously broken to $\text{SL}(2, \mathbb{R})$

3.2 Reparameterizations

Unfortunately, the conformal limit is inconsistent. While part of the four-point function has a finite part in the limit, known as the "conformal four-point function", another piece yields infinity, as will be seen in Section 3.3. This forces us to include the leading non-conformal contribution to the action, leading to a parametrically large $O(\beta J)$ term in the four-point function. This means that we are including the leading effects from the ∂_τ term, explicitly breaking the reparameterization symmetry in Equation 3.5.

In this limit, the leading solution to the Schwinger-Dyson equations at a given

temperature is still found by reparameterizing the zero-temperature solution $G_{\beta=\infty}$, but only $g(\tau) = \tau$ is a saddle point:

$$G_c(\tau_1, \tau_2) = G_{\beta=\infty}(e^{\frac{2\pi i}{\beta}\tau_1}, e^{\frac{2\pi i}{\beta}\tau_2})|(e^{\frac{2\pi i}{\beta}\tau_1})'|^{\Delta}|(e^{\frac{2\pi i}{\beta}\tau_2})'|^{\Delta}. \tag{3.7}$$

We call this the conformal two-point function. Including the leading effects from breaking reparameterization symmetry means that the reparameterization modes $g(\tau)$ become pseudo-Nambu-Goldstone modes, or soft modes. Thus we can write the leading action for Equation 3.3 by considering fluctuations away from the conformal Green's function generated by the reparameterization modes. For infinitesimal fluctuations $g(\tau) = \tau + \epsilon(\tau)$, the fluctuation in the correlator is

$$\delta_\epsilon G_c(\tau_1, \tau_2) = (\Delta\epsilon'(\tau_1) + \Delta\epsilon'(\tau_2) + \epsilon(\tau_1)\partial_{\tau_1} + \epsilon(\tau_2)\partial_{\tau_2})G_c(\tau_1, \tau_2), \tag{3.8}$$

and the corresponding action is

$$S \approx S_l = \frac{N\alpha_S}{\mathcal{J}} \int d\tau \frac{1}{2}(\epsilon''^2 - \lambda^2\epsilon'^2), \tag{3.9}$$

where α_S is a constant determined by q and numerical data (see [6],[17] for more details). The action for finite reparameterizations can be determined as well, yielding the Schwarzian action,

$$S_l = -\frac{N\alpha_S}{\mathcal{J}} \int_0^\beta d\tau \, \mathrm{Sch}(e^{\frac{2\pi i}{\beta}g(\tau)}, \tau), \quad \mathrm{Sch}(f(t), t) = \frac{f'''(t)}{f'(t)} - \frac{3}{2}\left(\frac{f''(t)}{f'(t)}\right)^2, \tag{3.10}$$

where we have defined the Schwarzian derivative. One can reproduce (3.9) by setting $g(\tau) = \tau + \epsilon(\tau)$ and expanding to quadratic order.

One important thing to note is that Equation 3.9 is zero for the reparameterizations $\epsilon(\tau) = e^{im\tau}, m = 0, \pm 1$. These are not true zero modes, but instead the result of an $\mathrm{SL}(2, \mathbb{R})$ gauge symmetry, coming from the fact that the conformal two-point function is unchanged by $\mathrm{SL}(2, \mathbb{R})$ transformations acting on $f = e^{\frac{2\pi i}{\beta}g(\tau)}$. Since we should only consider fluctuations leading to physically distinct configurations, such reparameterizations are gauge transformations.

Another important thing to note about these reparameterization modes is that they are actually the hydrodynamic modes of the system, up to a constant, making

the Schwarzian theory a hydrodynamic theory. One way to see this is that they represent a mapping from physical time, τ, into a "fluid time" $g(\tau)$. Another way is that the Schwarzian action, analytically continued to the Schwinger-Keldysh contour, is an example of a model with a Lagrangian of the form in Equation 2.12. Appendix B of [1] explicitly shows how one can obtain the Schwarzian action in Lorentzian time from the general hydrodynamic effective action; they find a hydrodynamic Lagrangian with a shift symmetry

$$\mathcal{L}_{\text{hydro}} = \mathcal{L}(\sigma_1) - \mathcal{L}(\sigma_2),\ \mathcal{L}(\sigma) = -a_2 \text{Sch}(e^{-\frac{2\pi}{\beta}\sigma}, t). \tag{3.11}$$

Under analytic continuation to Euclidean time, $-\sigma = ig$, and the shift symmetry is just a subset of the full $\text{SL}(2,\mathbb{R})$ symmetry.

We can write the Schwarzian action another way[1], which will be more useful when we consider the NLO corrections;

$$S_l = -N\alpha_S\varepsilon \int_0^{2\pi} d\theta\ \text{Sch}(e^{i\varphi(\theta)}, \theta), \tag{3.12}$$

where $\varepsilon = \frac{2\pi}{\beta J}$,$\theta = \frac{2\pi}{\beta}\tau$, and $\varphi(\theta) = \frac{2\pi}{\beta} g(\frac{\beta\theta}{2\pi})$ is a diffeomorphism of the unit circle.

In summary, the leading action for the SYK model comes from the explicit breaking of reparameterization invariance, and is characterized by a single gapless reparameterization mode that is equivalent to the hydrodynamic mode of Chapter 2.

3.3 Four point function

(3.8) and (3.9) can be used to find the Lorentzian connected four point function, both in time-ordered and out-of-time-ordered configurations, by finding the Euclidean time-ordered, averaged, connected four-point function,

$$\frac{1}{N}\mathcal{F}(\tau_1,\tau_2,\tau_3,\tau_4) \coloneqq \frac{1}{N^2}\sum_{i,j}\langle T\psi_i(\tau_1)\psi_i(\tau_2)\psi_j(\tau_3)\psi_j(\tau_4)\rangle - G(\tau_{12})G(\tau_{34}),\ \tau_{ij} \coloneqq \tau_i - \tau_j, \tag{3.13}$$

where we have subtracted off the disconnected piece and noted the N scaling of the connected piece. This can be found using Feynman diagrams, and is a sum of

[1] This is the convention found in [17]

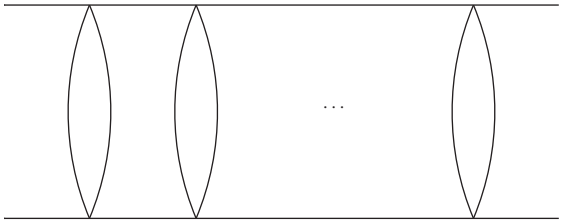

Figure 3.2: A Feynman diagram of the n^{th} term in the four-point function. Each rung contains $q-2$ lines in the general case.

ladder diagrams generated by a kernel $K(\tau_1, \cdots, \tau_4)$:

$$\mathcal{F} = \sum_{n=0}^{\infty} K^n \mathcal{F}_0, \quad \mathcal{F}_0 = -G(\tau_{13})G(\tau_{24}) + G(\tau_{14})G(\tau_{23}), \tag{3.14}$$

$$K(\tau_1, \cdots, \tau_4) = -J^2(q-1)G(\tau_{13})G(\tau_{24})G(\tau_{34})^{q-2}, \tag{3.15}$$

represented diagrammatically in Figure 3.2. This is the starting point in [6], where they solve this equation directly by diagonalizing the kernel and taking into consideration the leading effects of the ∂_τ term.

An alternative method is to note that, using Equation 3.3, we can find $\mathcal{F}$ near the conformal limit using

$$\mathcal{F}(\tau_1, \tau_2, \tau_3, \tau_4) = \langle \big(\widetilde{G}(\tau_{12}) - G_c(\tau_{12})\big)\big(\widetilde{G}(\tau_{34}) - G_c(\tau_{34})\big)\rangle, ^2 \tag{3.16}$$

i.e., by looking at the two-point function between fluctuations around the conformal correlator. Since we know that near the conformal limit, reparameterizations ought to be the most dominant, we look at the part of the connected four-point function that comes from infinitesimal reparameterizations,

$$\mathcal{F}(\tau_1, \tau_2, \tau_3, \tau_4)^{(-1)} = \langle \delta_\epsilon G_c(\tau_1, \tau_2)\delta_\epsilon G_c(\tau_3, \tau_4)\rangle, \tag{3.17}$$

where the (-1) superscript indicates the order in $1/\beta J$ we will end up finding. We can now use Equation 3.9 to obtain the correlator for ϵ and find $\mathcal{F}^{(-1)}$; to leading order the result only depends on two point functions of ϵ. The final expression

[2]Recall that $\widetilde{G}$ represent the integration variable found in the path integral of Equation 3.3.

differs depending on whether the time-ordering from Equation 3.13 results in $iijj$ order or $ijij$ order; the former yields

$$\frac{\mathcal{F}(\tau_1,\tau_2,\tau_3,\tau_4)^{(-1)}}{G(\tau_{12})G(\tau_{34})} = c\beta\mathcal{J}\left(\frac{\pi\tau_{12}}{\beta\tan\frac{\pi\tau_{12}}{\beta}}-1\right)\left(\frac{\pi\tau_{34}}{\beta\tan\frac{\pi\tau_{34}}{\beta}}-1\right), \tag{3.18}$$

where c is some constant. We now see why the conformal limit is inconsistent; setting $\beta J = \infty$ means Equation 3.18 diverges.

This expression can be analytically continued to a real time TOC by setting $\tau_i = \delta_i - it_i, \delta_1 > \cdots > \delta_4$, where the δ_i are simple regulators imposing the time-ordering. Doing so shows there is no exponential growth in the TOC; if $\tau_1 \approx \tau_2 \approx -it, \tau_3 \approx \tau_4 \approx i0$ as in Equation 2.31, then all of the terms in Equation 3.18 have finite limits as $t \to \infty$.

The $ijij$ ordering takes a simple expression when setting $\tau_3 = 0, \tau_3 = \frac{\beta}{2}$:

$$\frac{\mathcal{F}(\tau_1,\tau_2,0,\frac{\beta}{2})^{(-1)}}{G_c(\tau_{12})G_c(\frac{\beta}{2})} = -c\beta\mathcal{J}\left(\frac{\pi\tau_{12}}{\beta\tan\frac{\pi\tau_{12}}{\beta}}-1-\pi\frac{\sin\frac{\pi\tau_{12}}{\beta}\sin\frac{\pi\tau_{34}}{\beta}}{|\sin\frac{\pi\tau_{12}}{\beta}}\right). \tag{3.19}$$

This formula is useful for obtaining a common variant of the OTOC,

$$\widetilde{C}(t) = \langle\rho^{1/4}\psi_i(t)\rho^{1/4}\psi_j(0)\rho^{1/4}\psi_i(t)\rho^{1/4}\psi_j(0)\rangle,\ \rho = e^{-\beta H}. \tag{3.20}$$

This correlator has the same late-time growth in the chaos limit, $t_r \ll t \ll t_s$, as the traditional OTOC from Equation 1.1, but has each operator moved a quarter around the thermal circle, making for easier calculations. We can obtain it from Equation 3.19 by setting $\theta_1 = \frac{-\beta}{4} - it$, $\theta_2 = \frac{\beta}{4} - it$: the result is

$$\widetilde{C}(t)^{(-1)} = c\beta\mathcal{J}\left(1-\cosh\frac{2\pi t}{\beta}\right)G_c(\frac{\beta}{2})G_c(\frac{\beta}{2}), \tag{3.21}$$

demonstrating the exponential growth of the OTOC with Lyapunov exponent $\lambda = \frac{2\pi}{\beta}$.

In summary, direct calculation of the four-point function in the SYK model can be calculated using the Schwarzian theory, establishing the theory as chaotic. It is a hydrodynamic theory with a shift symmetry, and as we will show in the next section, satisfies the 0 + 1 dimensional version of pole-skipping.

Chapter 4

Energy Two-Point Function

We are now ready to calculate the SYK energy two-point function to leading order in $1/\beta J$. We will start by obtaining an explicit expression for the energy density $E(\tau)$ for the action in (3.10), along with the leading order in $\epsilon(\tau)$ contribution. This, along with the correlator for Fourier modes of $\epsilon(\tau)$, will give us the energy Matsubara correlator in frequency and time, which can be analytically continued to obtain various real time correlators. [1]

We will then calculate the energy two-point function for a generic hydrodynamic action with no spatial dependence, specializing to the SYK model afterwards and checking for agreement with the direct result.

4.1 SYK Direct Calculation

The action in (3.10) has time translation symmetry, yielding the Noether current for the energy,

$$E(\tau)^{(1)} = -B\Big(\frac{g'''}{g'} - \frac{3}{2}\big(\frac{g''}{g'}\big)^2 + \frac{\lambda^2}{2}g'^2\Big) = -B\ \mathrm{Sch}(\tan\frac{\pi g(\tau)}{\beta}, \tau), \tag{4.1}$$

where $B = N\alpha_s/\mathcal{J}$, and the superscript indicates we are at $O(1/\beta J)$.

Considering infinitesimal reparameterizations $g = \tau + \epsilon(\tau)$ and expanding to leading order in ϵ, neglecting total derivative terms, we get the quadratic action

[1] See Appendix B for details on thermal correlators.

(3.9) and energy

$$E^{(1)} = -B(\epsilon''' + \lambda^2\epsilon'). \tag{4.2}$$

To derive the two-point function for the energy density, we first obtain the two-point function for the Fourier modes of infinitesimal reparameterizations:

$$\begin{aligned} \epsilon &= \sum_{m\in\mathbb{Z}} \epsilon_m e^{-i\omega_m\tau}, \\ S_l &= \frac{1}{2}B\sum_m \beta\omega_m^2(\omega_m^2-\lambda^2)\epsilon_m\epsilon_{-m}, \\ \therefore \langle\epsilon_m\epsilon_n\rangle &= \frac{1}{B\beta}\frac{\delta_{m+n}}{\omega_m^2(\omega_m^2-\lambda^2)}, \end{aligned} \tag{4.3}$$

where $\omega_m = 2\pi n/\beta = \lambda m$ are Matsubara frequencies. It is important to note that the $SL(2,\mathbb{R})$ gauge symmetry is generated by the $m = 0, \pm 1$ Fourier modes of ϵ. Thus we can gauge-fix the action by simply dropping these modes, i.e., we set $\epsilon_0 = \epsilon_{\pm 1} = 0$, yielding a finite correlator for all valid m.

With this, the Matsubara correlator for the energy can be obtained:

$$\begin{aligned} E(i\omega_m)^{(1)} &= -iB\omega_m(\omega_m^2-\lambda^2)\epsilon_n, \\ G_M^{EE}(i\omega_m)^{(1)} &= \frac{B}{\beta}(\omega_m^2-\lambda^2), \\ \langle E(\tau)E(0)\rangle^{(1)} &= \sum_{m\neq 0,\pm 1} G_M^{EE}(i\omega_m)e^{-i\omega_m\tau} = \frac{N\alpha_S(2\pi)^2}{\mathcal{J}\beta^3}[1-\beta(\delta''(\tau)+\delta(\tau))]. \end{aligned} \tag{4.4}$$

After dropping contact terms, this yields a constant energy two-point function, the expected result for a conserved charge. Interestingly, it yields the same result as

$$\langle(\delta E)^2\rangle = \partial_\beta^2 \log Z = \frac{c}{\beta^3}, \tag{4.5}$$

where $c/\beta = (2\pi)^2\alpha_S N/\beta\mathcal{J}$ is the specific heat. This result leads to the surprising statement that the leading order connected four point function in the time-ordered

[2] $\log Z = -\beta E_0 + S_0 + \frac{c}{2\beta}$, where E_0, S_0 are the ground state energy and zero temperature entropy respectively. See [6], Section 2.6 for details.

configuration comes entirely from energy fluctuations. Using the result from [6] (Equation 3.129) and calculating the variation in the conformal correlator produced by variations in β, along with the saddle point relation $E = c/2\beta^2$, one obtains

$$\frac{\mathcal{F}^{(-1)}}{N} = \partial_\beta G(\tau_1, \tau_2)\partial_\beta G(\tau_3, \tau_4)\frac{\beta^6}{c^2}\langle T(\tau)T(0)\rangle^{(1)}, \tag{4.6}$$

where $\tau = \frac{1}{2}(\tau_1 + \tau_2 - \tau_3 - \tau_4)$

4.2 Hydrodynamics in 0+1 dimensions

We now calculate the retarded energy two-point function for a hydrodynamic EFT with no spatial dependence, $G_R^{EE}(t) = i\langle E_r(t)E_a(0)\rangle$. The theory is formulated on the the CTP contour in real time, and we have $E_r = \frac{1}{2}(E_1 + E_2)$, $E_a = E_1 - E_2$. We will then use this to find the energy two-point function for the SYK model.

We start by considering a general hydrodynamic Lagrangian with no spatial dependence to quadratic order; this can be obtained from (2.12) by setting all spatial derivatives equal to zero:

$$\mathcal{L}_{\text{hydro}} = \beta\epsilon_a f_1 \partial_t^2 \epsilon_r - \frac{i}{2}\epsilon_a M_1 \partial_t^2 \epsilon_a. \tag{4.7}$$

(Note that we have dropped the subscript from β_0, for consistency with the expressions in Chapter 3.

Using the results from [1], Appendix A, where $f_1^*(\partial_t) \coloneqq f_1(-\partial_t)$ is the operator obtained by doing integration by parts for f, we obtain the retarded energy two-point function for a general hydrodynamic action with no spatial dependence, as well as the two-point function whenever the action has a shift symmetry:

$$\begin{aligned} G_R^{EE}(t_1 - t_2) &= \beta^2 f_1(\partial_{t_1}) f_1^*(\partial_{t_2})\partial_{t_1}\partial_{t_2} G_R(t_1 - t_2) \\ &= -\beta^2(\partial_t - \lambda)^2 a(\partial_t)^2 \partial_t^2 G_R(t), \end{aligned} \tag{4.8}$$

where $G_R(t) = i\langle\epsilon_r(t)\epsilon_a(0)\rangle$ is the propagator of near-equilibrium hydrodynamic modes, $t \coloneqq t_1 - t_2$.

Dropping all spatial dependence for 2.19, we find $G_R(\omega) = -\frac{1}{\beta}\left(i\beta\omega^2 a(\omega)(\omega - i\lambda)\right)^{-1}$,

and so [3]

$$G_R^{EE}(\omega) = -i(\omega - i\lambda)a(\omega). \tag{4.9}$$

This is the $0+1$ dimensional version of pole-skipping: a hydrodynamic theory with shift symmetry possesses an energy two-point function that vanishes at $\omega = i\lambda$.

We now consider the SYK model, whose hydrodynamic Lagrangian (the Schwarzian action of the reparameterization modes) contains a shift symmetry. Recall that the Lagrangian that yields the Schwarzian action on two legs of a CTP contour is Equation 3.11; one finds that $f_1 = \frac{B}{\beta}(\partial_t - \lambda)(\partial_t + \lambda)$, yielding

$$\begin{aligned} G_R^{EE}(\omega) &= -\frac{B}{\beta}(\omega^2 + \lambda^2), \\ G_M^{EE}(i\omega_m) &= \frac{B}{\beta}(\omega_m^2 - \lambda^2). \end{aligned} \tag{4.10}$$

where in the last line we have analytically continued the retarded, real frequency correlator to give the Matsubara frequency correlator, $\omega \to i\omega_m$ (see Equation B.5). This is equal to the result from the direct SYK calculation, Equation 4.4.

In summary, we have found the leading order retarded energy two-point function for the SYKmodel, and found that it satisfies the $0 + 1$ dimensional version of pole-skipping, i.e., it possesses a zero at $\omega = i\lambda$. Since it is also a hydrodynamic theory, as shown in Section 3.2, the SYK model satisfies the conjecture. We now aim to investigate the model at NLO, and see if the model continues to satisfy the conjecture.

[3] We have inserted a factor of β into the definition of the Fourier transform, compared to [1], for consistency with our definition of the discrete Fourier series in Equation 4.3.

Chapter 5

Next-to-Leading Order Corrections

In this chapter, we investigate the NLO correction to the SYK action for the reparameterization mode, derived in [17]. We will calculate the retarded energy two-point function at NLO and look for its zeros, demonstrating that even at NLO the soft mode theory is maximally chaotic, thus satisfying the conjecture. We then show how to consistently incorporate the remaining degrees of freedom of the SYK model, establish their role in reducing the Lyapunov exponent, and comment on the difficulty in interpreting the theory as hydrodynamic.

The correction to the soft mode action retains the non-locality present in Equation 3.3; it reads

$$S_{\text{nl}} = -\frac{N\gamma\varepsilon^2}{2}\left[\iint \frac{d\theta_1}{2\pi}\frac{d\theta_2}{2\pi}\frac{\varphi'(\theta_1)^2\varphi'(\theta_2)^2}{\varphi_{12}^4}\left(\ln\left(\frac{\varphi_{12}^2}{\varphi'(\theta_1)\varphi'(\theta_2)\varepsilon^2}\right)+c\right)\right]_{\text{fin}}, \tag{5.1}$$

$$\varphi_{12} \coloneqq 2\sin\frac{\varphi(\theta_1)-\varphi(\theta_2)}{2}.$$ [1]

Here and in the following, we will use the field definition and angular time coordinate as in Equation 3.12; φ is the reparameterization mode, $\theta \in [0, 2\pi)$ is the

[1] Note that in this section, the subscript ij no longer means just the difference: $\theta_{12} = 2\sin\frac{\theta_1-\theta_2}{2}$. This is due to the prevalence of terms such as this when investigating the NLO soft mode theory. Differences such as $\theta_1 - \theta_2$ will be explicitly written out, or denoted by θ_- when appropriate.

(angular) time coordinate, and $\varepsilon = \frac{2\pi}{\beta J}$. The constant γ is related to α_S, c is a constant determined by the method chosen to regularize the ∂_τ perturbation in Equation 3.3, and the "fin" subscript indicates that we regularize the action by discarding any cutoff-dependent local terms that arise when one imposes a cutoff to regularize the φ_{12} divergence.[2] This action is $\mathrm{SL}(2,\mathbb{R})$ invariant, just as Equation 3.12 is, implying a shift symmetry; under the transformation $e^{i\varphi} \to e^{i\varphi} + \delta$, the variation of the Lagrangian vanishes.

5.1 NLO Corrections Summary

Let us discuss the origin of the non-local action. The ∂_τ term in Equation 3.3 is an irrelevant perturbation that produces UV corrections to the Green's function. The procedure in [17] is to replace this perturbation with a simpler UV perturbation, possessing a non-singular integral kernel $\sigma(\tau_1, \tau_2)$, and match the leading IR response of this perturbation to the numerical result from solving the full Schwinger-Dyson equations. This provides an analytically tractable way to determine the NLO action for the soft mode, along with corrections to the soft mode propagator and the four-point function, Equation 3.13.

After replacing the ∂_τ term with $\sigma(\tau_1, \tau_2)$, redefining our variables as in Table 5.1, and expanding to quadratic order in fluctuations around the conformal saddle point, $(\widetilde{G}, \widetilde{\Sigma}) \to (\widetilde{G}_c + \delta\widetilde{G}, \widetilde{\Sigma}_c + \delta\widetilde{\Sigma})$, Equation 3.3 becomes

$$\frac{I[\delta\widetilde{G}, \delta\widetilde{\Sigma}]}{N} \approx \frac{1}{4}\mathrm{Tr}(\widetilde{G}_c \delta\widetilde{\Sigma})^2 + \frac{1}{2}\int d\varphi_1\, d\varphi_2 \Big(\delta\widetilde{\Sigma}(\varphi_1,\varphi_2)\delta\widetilde{G}(\varphi_1,\varphi_2) - \frac{q-1}{2}|\widetilde{G}_c(\varphi_1,\varphi_2)|^{q-2}\delta\widetilde{G}(\varphi_1,\varphi_2)^2 - \widetilde{\sigma}(\varphi_1,\varphi_2)(\widetilde{G}_c(\varphi_1,\varphi_2) + \delta\widetilde{G}(\varphi_1,\varphi_2))\Big).^3 \tag{5.2}$$

The action here has been expressed in a frame-invariant way, using $\varphi(\theta)$ as a time variable as opposed to the physical time θ (recall that φ is a generic diffeomorphism on S^1, which will later represent the reparameterization mode). We can now set $\delta\widetilde{\Sigma}$ equal to its saddle point to get an action for $\delta\widetilde{G}$, and subsequently set $\delta\widetilde{G}$ equal to

[2] This procedure is actually unique, as argued in [17]

[3] See Table 5.1 for a definition of the symbols used throughout this chapter. These symbols are defined for consistency with [17].

its saddle point, resulting in (after another change of variables)

$$\frac{I[\delta g]}{N} = -\frac{1}{2}\langle s|g_c + \delta g\rangle + \frac{1}{4}\langle \delta g|K_c^{-1} - 1|\delta g\rangle, \tag{5.3a}$$

$$\frac{I_*}{N} = -\frac{1}{2}\langle s|g_c\rangle - \frac{1}{4}\langle s|K_c(K_c-1)^{-1}|s\rangle, \tag{5.3b}$$

where I_* is the action evaluated at the saddle point for a given UV perturbation σ, and K_c is the "conformal kernel", which is a symmetrized version of the kernel from Equation 3.15 evaluated in the conformal limit; see Table 5.1 for the definition. The inner products are defined as integrals over $S^1 \times S^1$, $\langle f|g\rangle \coloneqq \int d\theta_1 d\theta_2 f(\theta_1,\theta_2)g(\theta_1,\theta_2)$, and $A|f\rangle \coloneqq \int d\theta_3 d\theta_4 A(\theta_1,\theta_2,\theta_3,\theta_4)f(\theta_3,\theta_4)$. Note that K_c has eigenfunctions with eigenvalue 1 generated by infinitesimal reparameterization modes $\delta\varphi$, $\delta\widetilde{G}^{||} = |G|^{\frac{q-2}{2}}\delta_{\delta\varphi}G_c$, where $\delta_{\delta\varphi}G_c$ was given in Equation 3.8. Hence, $K_c(K_c-1)^{-1}$ is only defined on the orthogonal complement of the reparameterization mode subspace, with elements labeled by $\delta\widetilde{G}^{\perp}$. The conformal kernel generates the conformal four-point function $\widetilde{\mathcal{F}}_c^{\perp}$, as calculated in [6].

The first term in Equation 5.3a generates the Schwarzian action Equation 3.12, while the second will lead to the NLO correction to the action, Equation 5.1. Meanwhile, the second term in Equation 5.3b is interpreted as giving a correction to the conformal Green's function for a given source, $\delta g_{UV} = \frac{1}{2}\frac{K_c}{K_c-1}|s\rangle$. These UV corrections to the Green's function have been found in the zero-temperature limit numerically for the exact ∂_τ source to be

$$\delta G_{UV}(\tau_1,\tau_2) \propto |J(\tau_1-\tau_2)|^{1-h}G_{\beta=\infty}(\tau_1,\tau_2),\ \text{Re}\ h \geq 1. \tag{5.4}$$

The next step is to choose an appropriate UV perturbation source $\sigma(\theta_1,\theta_2)$ (or equivalently $s(\theta_1,\theta_2)$) that reproduces the UV corrections to the Green's function, in order to facilitate calculation of the second term in Equation 5.3a. The source should only be supported for $|\theta_1-\theta_2| \ll 1$, while still impacting the IR properties of the model. Any source can be expressed in the basis of eigenfunctions of the conformal kernel, $W_h(\theta_1,\theta_2)$ (each with eigenvalue $k_c(h)$), multiplied by a smooth window function $u(\xi \coloneqq \ln\frac{|\theta_1-\theta_2|}{\varepsilon})$, which provides the proper support. Terms with $k_c(h) \neq 1$ only contribute at short times, as $\frac{K_c}{1-K_c}|uW_h\rangle$ will only

Symbol	Meaning	Analytic Expression
$\varepsilon_\varphi(\varphi)$	Renormalizing field representing the soft mode in a given frame	$\varepsilon \frac{d\varphi}{d\theta}$
$\widetilde{G}_\varphi(\varphi_1, \varphi_2)$	Renormalized Green's function in a given frame	$G(\tau_1, \tau_2) = \widetilde{G}(\varphi_1, \varphi_2)(\varepsilon_\varphi(\varphi_1))^\Delta(\varepsilon_\varphi(\varphi_2))^\Delta$
$\widetilde{G}_c(\theta_1, \theta_2)$	Renormalized conformal Green's function	$\widetilde{G}_{\varphi(\theta)=\theta}(\theta_1, \theta_2)$
$\widetilde{\Sigma}_\varphi(\varphi_1, \varphi_2)$	Renormalized and redefined self-energy	$\Sigma(\tau_1, \tau_2) = J^2(\widetilde{\Sigma}_\varphi(\varphi_1, \varphi_2)$ $-\widetilde{\sigma}_\varphi(\varphi_1, \varphi_2))(\varepsilon_\varphi(\varphi_1))^{1-\Delta}(\varepsilon_\varphi(\varphi_2))^{1-\Delta}$
$\widetilde{\sigma}_\varphi(\varphi_1, \varphi_2)$	Renormalized perturbation source	$\sigma(\tau_1, \tau_2) = J^2\widetilde{\sigma}_\varphi(\varphi_1, \varphi_2)(\varepsilon_\varphi(\varphi_1))^{1-\Delta}(\varepsilon_\varphi(\varphi_2))^{1-\Delta}$
$R_c(\varphi_1, \varphi_2)$	Common function	$(q-1)^{1/2}\lvert\widetilde{G}_c(\varphi_1, \varphi_2)\rvert^{\frac{q-2}{2}}$
$g(\varphi_1, \varphi_2)$	Normalized two-point function	$R_c(\varphi_1, \varphi_2)\widetilde{G}(\varphi_1, \varphi_2)$
$s(\varphi_1, \varphi_2)$	Normalized source	$R_c(\varphi_1, \varphi_2)^{-1}\widetilde{\sigma}(\varphi_1, \varphi_2)$
$K_c(\varphi_1, \varphi_2; \varphi_3, \varphi_4)$	Kernel for 4-point function in conformal limit	$R_c(\varphi_1, \varphi_2)\widetilde{G}_c(\varphi_1, \varphi_3)\widetilde{G}_c(\varphi_4, \varphi_2)R_c(\varphi_3, \varphi_4)$
$\widetilde{\mathcal{F}}_c^\perp(\varphi_1, \varphi_2; \varphi_3, \varphi_4)$	Conformal four-point function	$R_c(\varphi_1, \varphi_2)^{-1}\big[\frac{K_c}{1-K_c}(\varphi_1, \varphi_2; \varphi_3, \varphi_4)$ $-\frac{K_c}{1-K_c}(\varphi_1, \varphi_2; \varphi_4, \varphi_3)\big]R_c(\varphi_3, \varphi_4)^{-1}$

Table 5.1: Various definitions used to obtain the non-local action for the soft mode.

be supported at short times. However, when $k_c(h_I) = 1$, we have a resonance; since $\frac{K_c}{1-K_c}|W_{h_I}\rangle = \frac{k_c(h_I)}{1-k_c(h_I)}|W_{h_I}\rangle = \infty$, including the window function means $\delta g_{UV} = \frac{1}{2}\frac{K_c}{1-K_c}|uW_{h_I}\rangle$ can affect the model at larger times. Thus, we consider sources corresponding to these eigenfunctions.

The source for a given solution of $k_c(h_I) = 1$ is

$$s_I(\theta_1, \theta_2) = -a_I \varepsilon^{h_I - 1} |\theta_1 - \theta_2|^{-h_I} \operatorname{sgn}(\theta_1 - \theta_2) u(\xi), \tag{5.5}$$

where a_I is a constant to be determine numerically, ε^{-h_I-1} is to provide proper units, and $|\theta_1 - \theta_2|^{-h_I}\operatorname{sgn}(\theta_1 - \theta_2)$ is an approximate eigenfunction of K_c. This yields

$$\delta g_{UV,I} \approx \frac{a_I}{-k_c'(h_I)} \varepsilon^{h_I - 1} |\theta_1 - \theta_2|^{-h_I} \operatorname{sgn}(\theta_1 - \theta_2). \tag{5.6}$$

This has the same form as Equation 5.4. The dominant source and response are given by $h_0 = 2$; this is the source we will use to derive Equation 5.1.

Finally, we can change our degrees of freedom to allow for easier calculations. Our primary degrees of freedom are represented by $\delta\widetilde{G}$, which separates into eigenfunctions of K_c with eigenvalue 1 and all other eigenvalues (the orthogonal compliment), $\delta\widetilde{G} = \delta\widetilde{G}^{||} + \delta\widetilde{G}^{\perp}$. To make calculations easier, for each $\delta\widetilde{G}$ we can change variables into a frame $\varphi(\theta)$ where $\delta\widetilde{G}^{||}_{\varphi} = 0$; this is called the "conformal frame". The advantage of this frame is that we've eliminated fluctuations where $\frac{K_c}{1-K_c}|\delta\widetilde{G}\rangle = \infty$. We can now use a variation of Equation 5.3a with calculations done in the conformal frame, allowing us to use the conformal kernel as defined on the orthogonal compliment:

$$\frac{S[\delta g^{\perp}_{\varphi}, \varphi]}{N} = -\frac{1}{2}\langle s_{\varphi}|g_c + \delta g^{\perp}_{\varphi}\rangle + \frac{1}{4}\langle \delta g^{\perp}_{\varphi}|K_c^{-1} - 1|\delta g^{\perp}_{\varphi}\rangle, \tag{5.7a}$$

$$\frac{S_*[\varphi]}{N} = -\frac{1}{2}\langle s_{\varphi}|g_c\rangle - \frac{1}{4}\langle s_{\varphi}|K_c(K_c - 1)^{-1}|s_{\varphi}\rangle, \tag{5.7b}$$

where all of the inner products are taken in the conformal frame, and in the second line we again set $\delta g^{\perp}_{\varphi}$ to its saddle point. Our remaining degree of freedom is the soft mode φ. Equation 5.1 can now be obtained from the second term of Equation 5.7b.

5.2 Energy Two-point Function

We now extend the results from Section 4.1 to NLO. Equation 5.1 is invariant under simultaneous translation of both times, and has an associated Noether current,

$$\begin{aligned} T_{\rm nl}(\theta_1,\theta_2) &= -\frac{N\gamma\varepsilon^2}{8\pi^2}\varphi_{12}^{-4}\left[\varphi'(\theta_1)^2\varphi'(\theta_2)^2\left(\ln\left(\frac{\varphi_{12}^2}{\varphi'(\theta_1)\varphi'(\theta_2)\varepsilon^2}\right)+c-1\right)\right], \\ T_{\rm nl}(\theta_1,\theta_2) &\approx -\frac{N\gamma\varepsilon^2}{8\pi^2}\theta_{12}^{-4}\Bigg[2\ln\theta_{12}-2\ln\varepsilon+c-1 \\ &\qquad +(4\ln\theta_{12}-4\ln\varepsilon+2c-3)\left(\delta\varphi_1'+\delta\varphi_2'-\frac{\delta\varphi_1-\delta\varphi_2}{\tan\frac{\theta_1-\theta_2}{2}}\right)\Bigg], \end{aligned} \tag{5.8}$$

where $(\partial_1+\partial_2)T_{\rm nl}=0$, and in the second line we expanded to linear order in $\delta\varphi=\varphi-\theta$.

We also find that the Noether current for the local action Equation 3.12 is

$$\begin{aligned} T_{\rm l}(\theta_+) &= -N\alpha_s\varepsilon\ \mathrm{Sch}(e^{i\varphi(\theta_+)},\theta_+), \\ T_{\rm l}(\theta_+) &\simeq -N\alpha_s\varepsilon\left(\frac{1}{2}+(\partial_{\theta_+}^3+\partial_{\theta_+})\delta\varphi(\theta_+)\right). \end{aligned} \tag{5.9}$$

where we use the fact that the Schwarzian is obtained with respect to the average of the two times, $\theta_+=\frac{\theta_1+\theta_2}{2}$, as shown in [17], Section 3.2. Note that the energy of the system from Section 4.1 is related to the generator of θ_+ translations by $E(\tau_+)=\lambda T(\frac{\theta_+}{\lambda})$, so $G_M^{EE}(i\omega_m)=\lambda^2\langle T_m T_{-m}\rangle$.

Now, for the contribution from the non-local action, we must integrate the current with respect to $\theta_- := \theta_1-\theta_2$ to obtain the generator of average-time translations. We can then calculate the $O(\varepsilon^2)$ part of the energy two-point function:

$$T(\theta_+) = T_{(\rm l)}(\theta_+)+\int\frac{d\theta_-}{2\pi}T_{(\rm nl)}(\theta_1,\theta_2)+O(\varepsilon^3) =: T_{(\rm l)}(\theta_+)+T_{(\rm nl)}(\theta_+), \tag{5.10}$$

$$\langle T(\theta_+)T(\theta_+')\rangle^{(2)} = \langle T_{(\rm l)}T_{(\rm l)}\rangle^{(0)}+\langle T_{(\rm l)}T_{(\rm nl)}\rangle^{(-1)}+\langle T_{(\rm nl)}T_{(\rm l)}\rangle^{(-1)}. \tag{5.11}$$

where the superscripts on the right-hand side indicate the order in ε of the correlator for the soft mode used: (-1) indicates the soft mode correlator in Equation 4.3, and (0) the correlator from the non-local action Equation 5.1. The local-local piece was

found in [17], Equation 197:

$$\langle T_{(\mathrm{l})_m} T_{(\mathrm{l})_{-m}} \rangle^{(0)} = -\frac{N\gamma\varepsilon^2}{4\pi^2}\left(\partial_h u_{h,m}\big|_{h=2} + (2\ln\varepsilon + 2 - c)u_{2,m} + \frac{1}{6} - \frac{1}{4}\delta_{m,0}\right). \tag{5.12}$$

We calculate the Fourier modes of the non-local-local piece, yielding

$$\langle T_{(\mathrm{l})_m} T_{(\mathrm{nl})_{-m}} \rangle^{(-1)} = -\frac{N\gamma\varepsilon^2}{8\pi^2}\left(-6\ln\varepsilon + 3c - \frac{9}{2} - \frac{8}{3}\partial_h\right)\left(u_{h,\frac{m}{2}} + u_{h,-\frac{m}{2}}\right)\big|_{h=2}, \tag{5.13}$$

where

$$u_{h,m} = \int_0^{2\pi} (2\sin\frac{\theta}{2})^{-2h} e^{im\theta}\frac{d\theta}{2\pi} = e^{i\pi m}\frac{\Gamma(1-2h)}{\Gamma(1-h+m)\Gamma(1-h-m)}. \tag{5.14}$$

We thus obtain the $O(\varepsilon^2)$ part of the energy Matsubara correlator:

$$\begin{aligned} G_M^{EE}(i\omega_m) = -\frac{N\gamma\varepsilon^2}{48\pi^2}\Bigg(&\frac{\omega_m}{\lambda}(\omega_m^2 - \lambda^2)\left[2\ln\varepsilon + 2 - c - 2\psi(4) + 2\psi\left(\frac{\omega_m}{\lambda} + 2\right)\right] \\ &- 3(\omega_m^2 - \lambda^2) - 3\lambda^2\delta_{m,0} + \cos^2\frac{\omega_m\pi}{2\lambda}\Bigg(\frac{\omega_m}{2\lambda}\left[\left(\frac{\omega_m}{2}\right)^2 - \lambda^2\right] \\ &\left[-6\ln\varepsilon + 3c - \frac{9}{2} - \frac{8}{3}\left(-2\psi(4) + 2\psi\left(\frac{\omega_m}{2\lambda} + 2\right)\right)\right] + 2\omega_m^2 - \frac{8}{3}\lambda^2\Bigg)\Bigg), \end{aligned} \tag{5.15}$$

where ψ is the digamma function. The expression is zero when $\omega_m = \lambda$, so on analytic continuation $G_R^{EE}(\omega = i\lambda) = 0$. According to the conjecture from 4.2, this should occur for a maximally chaotic theory; indeed, [17] found that at NLO the soft mode contribution to the exponentially growing part of the OTOC at is

$$\mathcal{F}^{(0)}_{\text{soft mode}}(\theta_1,\theta_2,\theta_3,\theta_4) \approx \frac{1}{(q-1)b}\Bigg[\theta_{12}\theta_{34} f^{\parallel}(\theta_1,\cdots,\theta_4) \\ - \frac{3}{(-k_c'(2))}\frac{1}{2\pi \sin\frac{\theta_1-\theta_2}{2}\sin\frac{\theta_3-\theta_4}{2}}\Bigg((\pi - 2\Delta\theta_+)\cos\Delta\theta_+ \\ + \left(2 - \frac{\pi-(\theta_1-\theta_2)}{\tan\frac{\theta_1-\theta_2}{2}} - \frac{\pi-(\theta_3-\theta_4)}{\tan\frac{\theta_3-\theta_4}{2}}\right)\sin\Delta\theta_+\Bigg)\Bigg], \tag{5.16}$$

where $\Delta\theta_+ = \frac{\theta_1+\theta_2-(\theta_3+\theta_4)}{2}$ and $f^{\parallel}$ is a (rather complicated) function that arises in the analysis; see [17], Section 5.1.5 for its exact form. This expression only includes the terms that grow exponentially upon analytic continuation to the time configuration from Equation 3.20.

To find any change in the Lyapunov exponent, we analytically continue Equation 5.16 to real time as we did in Section 3.3 and look for terms that go like $te^{\frac{2\pi}{\beta}t}$; these correspond to adding a small negative correction to the Lyapunov exponent in Equation 3.21, as

$$e^{\left(\frac{2\pi}{\beta}-\frac{1}{\beta J}\delta\lambda\right)t} \approx e^{\frac{2\pi}{\beta}t}\left(1 - \frac{1}{\beta J}\delta\lambda t\right). \tag{5.17}$$

While at first glance it appears there are terms proportional to $te^{\frac{2\pi}{\beta}t}$ in Equation 5.16 (e.g., the $\Delta\theta_+\cos\Delta\theta_+$ term), we have explicitly checked that $f^{\parallel}$ contains terms that directly cancels them. Thus the exponential growth remains proportional to $e^{\frac{2\pi}{\beta}t}$.

This confirms the fact that the correction to the soft mode action does not change the Lyapunov exponent. This makes sense when considering the symmetries of the theory: the soft mode action must be $\mathrm{SL}(2,\mathbb{R})$ invariant to all orders in perturbation theory, as it's a gauge symmetry, causing the maximally chaotic behaviour. Since the soft mode still maintains its status as a hydrodynamic mode, the soft mode sector of the SYK model at NLO satisfies the conjecture.

5.3 Orthogonal Modes

The conclusion of the previous section supports the shift symmetry conjecture, demonstrating another example of a maximally chaotic theory with a shift symmetry. However, it doesn't achieve our goal of checking the conjecture for a near-maximally chaotic theory. It is known that the SYK model is only maximally chaotic at leading order; at NLO the Lyapunov exponent receives a negative correction. The soft mode action in 5.1 yielded a maximal Lyapunov exponent. What's missing?

The answer lies in the step from Equation 5.7a to Equation 5.7b, where we set $\delta g_\perp$ equal to its saddle point. This means that in Equation 5.7b, we are only looking at fluctuations in the two-point function generated by the reparameterization mode, and nothing else. However, these are not all possible fluctuations, and it is these other "orthogonal modes" that reduce the Lyapunov exponent. This was first noted in [6], whose authors calculated the conformal four-point function from Table 5.1 by diagonalizing the kernel K (excluding the eigenfunctions corresponding to the reparameterization mode) and demonstrated that it contains a term proportional to $te^{\frac{2\pi}{\beta}t}$. We will now show how to consistently incorporate the orthogonal modes with the soft mode theory, reproducing the conformal four-point function.

We start with the action Equation 5.7a, restated here for convenience:

$$S[\delta g^\perp, \varphi] = -\frac{1}{2}\langle s_\varphi | g_c + \delta g^\perp\rangle + \frac{1}{4}\langle \delta g^\perp | K_c^{-1} - 1 | \delta g^\perp\rangle.$$

Recall that the φ dependence is encoded in the fact that the integrals are taken with respect to $\varphi \coloneqq \varphi(\theta)$. We now replace $\delta g^\perp$ with its saddle point plus fluctuations, $\delta g^\perp = \delta g^\perp_* + \eta$; one finds $\delta g^\perp_* = -\frac{1}{2}\frac{K_c}{K_c - 1}|s_\varphi\rangle$, and

$$\begin{aligned} S[\eta, \varphi] &= -\frac{1}{2}\langle s_\varphi | g_c\rangle - \frac{1}{4}\langle s_\varphi | K_c(K_c - 1^{-1})|s_\varphi\rangle + \frac{1}{4}\langle \eta | K_c^{-1} - 1 | \eta\rangle \\ &= S_{\mathrm{l}}[\varphi] + S_{\mathrm{nl}}[\varphi] + S_\perp[\eta, \varphi]. \end{aligned} \tag{5.18}$$

The first term yields the Schwarzian, the second yields the non-local correction to the soft mode action, and the final yields the action for the orthogonal modes, which represent all fluctuations of the two point function away from the saddle point that are not generated by reparameterizations.

Explicitly, the action for the orthogonal modes, including their coupling to the soft mode, is

$$\begin{aligned} S_\perp[\eta,\varphi] =& \frac{1}{4}\int d\varphi_1 d\varphi_2 d\varphi_3 d\varphi_4 \eta(\varphi_1,\varphi_2)\left[K_c^{-1}(\varphi_1,...,\varphi_4) - 1(\varphi_1,...,\varphi_4)\right]\eta(\varphi_3,\varphi_4) \\ =& \frac{1}{4}\int d\theta_1 d\theta_2 d\theta_3 d\theta_4 \eta(\theta_1,\theta_2)\Bigg[K_c^{-1}(\theta_1,...,\theta_4)\left(\prod_i \varphi'(\theta_i)\right) \\ & - 1(\theta_1,...,\theta_4)\Bigg]\eta(\theta_3,\theta_4), \end{aligned} \tag{5.19}$$

where in the last line we have switched to the physical frame, where the transformation of K_c and η under reparameterizations was determined via their relationship to the original two-point function. $1(\theta_1,\theta_2,\theta_3,\theta_4)$ is the kernel of the identity operator on antisymmetric functions.

We can easily find the two-point function of orthogonal modes, since Equation 5.19 is Gaussian with respect to $\eta(\theta_1,\theta_2)$. If $S_\perp$ was a function of $\eta(\theta_1,\theta_2)$ only, then the two-point function would just be the inverse-kernel, $(K_c^{-1}-1)^{-1}$. But since Equation 5.19 does have φ dependence, we must take the expectation value with respect to φ of the inverse-kernel:

$$\langle\eta(\theta_1,\theta_2)\eta(\theta_3,\theta_4)\rangle = \langle 2\left[K_c^{-1}(\theta_1,...,\theta_4)\left(\prod_i \varphi'(\theta_i)\right) - 1(\theta_1,...,\theta_4)\right]^{-1}\rangle_\varphi. \tag{5.20}$$

Using the antisymmetry of Equation 5.19, we can also write it in an antisymmetrized form:

$$\begin{aligned} \langle\eta(\theta_1,\theta_2)\eta(\theta_3,\theta_4)\rangle =& \Bigg\langle\left[K_c^{-1}(\theta_1,\theta_2;\theta_3,\theta_4)\left(\prod_i \varphi'(\theta_i)\right) - 1(\theta_1,\theta_2;\theta_3,\theta_4)\right]^{-1} \\ & - \left[K_c^{-1}(\theta_1,\theta_2;\theta_4,\theta_3)\left(\prod_i \varphi'(\theta_i)\right) - 1(\theta_1,\theta_2;\theta_4,\theta_3)\right]^{-1}\Bigg\rangle_\varphi. \end{aligned} \tag{5.21}$$

However, note that if we set $\varphi(\theta)$ to the identity, we reproduce the conformal

four-point function:

$$\begin{aligned}\langle \eta(\theta_1,\theta_2)\eta(\theta_3,\theta_4)\rangle &= \frac{K_c}{K_c-1}(\theta_1,\theta_2;\theta_3,\theta_4) - \frac{K_c}{K_c-1}(\theta_1,\theta_2;\theta_4,\theta_3) \\ &= R_c(\theta_1,\theta_2)\widetilde{\mathcal{F}}_c^{\perp}(\theta_1,\theta_2,\theta_3,\theta_4)R_c(\theta_3,\theta_4).\end{aligned} \tag{5.22}$$

As shown in [6], this is already leading order in $1/N$. This implies that including the effects of the fluctuating soft mode will be lower order in $1/N$, since the soft mode propagator is $O(N^{-1})$. This justifies setting $\varphi(\theta) = \theta$; the orthogonal and soft modes decouple.

Finally, since $\delta\widetilde{G}^{\perp} = R_c^{-1}\eta$ are the fluctuations due to orthogonal modes,

$$\langle \delta\widetilde{G}^{\perp}(\theta_1,\theta_2)\delta\widetilde{G}^{\perp}(\theta_3,\theta_4)\rangle = \widetilde{\mathcal{F}}_c^{\perp}(\theta_1,\theta_2,\theta_4,\theta_3). \tag{5.23}$$

Thus, by including fluctuations in the two-point function due to orthogonal modes, we have properly reproduced the conformal four-point function. This is added to the contribution from the soft mode in Equation 5.16 to give the full NLO four-point function. As [6] showed, it is this piece of the four-point function that is responsible for the reduction of the Lyapunov exponent; in the chaos limit $t_r \ll t \ll t_s$, it contributes an $O((\beta J)^0)$ term proportional to $te^{\frac{2\pi}{\beta}t}$.

The orthogonal modes can be characterized by their eigenvalue $h(h-1)$ with the conformal casimir, thanks to the conformal symmetry of K_c. There are infinitely many such values of h; a discrete subset $h = 2n, n \geq 2$, and a continuum piece $h = \frac{1}{2} + is$. While the continuum subset is unimportant in the chaos limit, one must sum over the entire discrete subset to get a convergent result. This is similar to how infinitely many stringy modes must be summed over for ADS black holes at NLO.

These orthogonal modes, unlike the soft mode, do not admit any sort of interpretation as hydrodynamic variables. For one, they parameterize all of the remaining degrees of freedom of the microscopic model near the saddle point; hydrodynamic modes, on the other hand, only parameterize the long-lived, gapless degrees of freedom. Additionally, there is no clear way to interpret even a subset of the orthogonal modes as mappings from physical spacetime to fluid spacetime, as is required for the description to be hydrodynamical. This suggests that another ingredient needs to be added to the conjectured hydrodynamic origin of chaos.

Chapter 6

Conclusion

The conjectured hydrodynamic origin of chaos, with shift symmetry as the cause and pole-skipping as a necessary condition, has been tested against another maximally chaotic theory and survived, but against a near-maximally chaotic theory it comes up short. After modifying the conjecture for theories with no spatial degrees of freedom, we predict that chaotic theories admit a hydrodynamic description, contain a shift symmetry, and possess a zero in the frequency space retarded energy two-point function at $\omega = i\lambda$. These all hold true for the SYK model at leading order, and we have demonstrated that they hold even at NLO in the soft mode sector. However, by carefully incorporating the other degrees of freedom of the SYK model, we see that the orthogonal modes reduce the Lyapunov exponent, decouple from the soft mode sector, and admit no clear hydrodynamic interpretation.

Understanding how to change the conjecture to correctly account for near-maximally chaotic theories is of paramount importance if we want to determine a universal origin of chaos. Several proposals have been made to this end; in [1] it is suggested that, similar to Regge physics, the infinitely many stringy modes mentioned in Section 5.3 might be captured by a single mode. In [18], it is suggested that a type of inelastic scattering between "stringy states" dominates the OTOCs, accurately describing even nearly-maximally chaotic theories like the SYK model. The possibility of treating the hydrodynamic theory as on open field theory as in [19] may also play a role in the reduction of chaos. By investigating these avenues, we hope to gain deeper understanding into the origin of chaos.

Bibliography

[1] M. Blake, H. Lee, and H. Liu, "A quantum hydrodynamical description for scrambling and many-body chaos," arXiv:1801.00010 [hep-th].

[2] A. I. Larkin and Y. N. Ovchinnikov, "Quasiclassical method in the theory of superconductivity," *Soviet Physics, JETP* (1969) 1200.

[3] J. Maldacena, S. H. Shenker, and D. Stanford, "A bound on chaos," *Journal of High Energy Physics* **2016** no. 8, (Aug, 2016) 106, arXiv:1503.01409 [hep-th]. https://doi.org/10.1007/JHEP08(2016)106.

[4] A. Kitaev, "Hidden correlations in the Hawking radiation and thermal noise.," 2015. http://online.kitp.ucsb.edu/online/joint98/kitaev/. Talks at KITP.

[5] S. H. Shenker and D. Stanford, "Stringy effects in scrambling," *Journal of High Energy Physics* **2015** no. 5, (May, 2015) 132, arXiv:1412.6087 [hep-th]. https://doi.org/10.1007/JHEP05(2015)132.

[6] J. Maldacena and D. Stanford, "Remarks on the Sachdev-Ye-Kitaev model," *Phys. Rev. D* **94** (Nov, 2016) 106002, arXiv:1604.07818 [hep-th]. https://link.aps.org/doi/10.1103/PhysRevD.94.106002.

[7] D. Stanford, "Many-body chaos at weak coupling," *Journal of High Energy Physics* **2016** no. 10, (Oct, 2016) 9, arXiv:1512.07687 [hep-th]. https://doi.org/10.1007/JHEP10(2016)009.

[8] Y. Gu, X.-L. Qi, and D. Stanford, "Local criticality, diffusion and chaos in generalized Sachdev-Ye-Kitaev models," *Journal of High Energy Physics* **2017** no. 5, (May, 2017) 125, arXiv:1609.07832 [hep-th]. https://doi.org/10.1007/JHEP05(2017)125.

[9] F. M. Haehl and M. Rozali, "Effective field theory for chaotic CFTs," *Journal of High Energy Physics* **2018** no. 10, (Oct, 2018) 118, arXiv:1808.02898 [hep-th]. https://doi.org/10.1007/JHEP10(2018)118.

[10] M. Blake, R. A. Davison, S. Grozdanov, and H. Liu, "Many-body chaos and energy dynamics in holography," *Journal of High Energy Physics* **2018** no. 10, (Oct, 2018) 35, arXiv:1809.01169 [hep-th]. https://doi.org/10.1007/JHEP10(2018)035.

[11] S. Grozdanov, "On the connection between hydrodynamics and quantum chaos in holographic theories with stringy corrections," *Journal of High Energy Physics* **2019** no. 1, (Jan, 2019) 48, arXiv:1811.09641 [hep-th]. https://doi.org/10.1007/JHEP01(2019)048.

[12] M. Crossley, G. Paolo, and H. Liu, "Effective field theory of dissipative fluids," arXiv:1511.03646 [hep-th].

[13] A. Kamenev, *Field Theory of Non-Equilibrium Systems*. Cambridge University Press, 2011.

[14] A. Kitaev, "A simple model of quantum holography," 2017. http://online.kitp.ucsb.edu/online/entangled15/kitaev/ and http://online.kitp.ucsb.edu/online/entangled15/kitaev2/.

[15] S. Sachdev and J. Ye, "Gapless spin-fluid ground state in a random quantum Heisenberg magnet," *Phys. Rev. Lett.* **70** (May, 1993) 3339–3342, arXiv:cond-mat/9212030. https://link.aps.org/doi/10.1103/PhysRevLett.70.3339.

[16] D. A. Roberts and D. Stanford, "Diagnosing chaos using four-point functions in two-dimensional conformal field theory," *Phys. Rev. Lett.* **115** (Sep, 2015) 131603, arXiv:1412.5123 [hep-th]. https://link.aps.org/doi/10.1103/PhysRevLett.115.131603.

[17] A. Kitaev and S. J. Suh, "The soft mode in the Sachdev-Ye-Kitaev model and its gravity dual," *Journal of High Energy Physics* **2018** no. 5, (May, 2018) 183, arXiv:1711.08467 [hep-th]. https://doi.org/10.1007/JHEP05(2018)183.

[18] Y. Gu and A. Kitaev, "On the relation between the magnitude and exponent of OTOCs," *Journal of High Energy Physics* **2019** no. 2, (Feb, 2019) 75, arXiv:1812.00120 [hep-th]. https://doi.org/10.1007/JHEP02(2019)075.

[19] Avinash, C. Jana, R. Loganayagam, and A. Rudra, "Renormalization in Open Quantum Field theory I: Scalar field theory," arXiv:1704.08335 [hep-th].

[20] L. M. Sieberer, M. Buchhold, and S. Diehl, "Keldysh field theory for driven open quantum systems," *Reports on Progress in Physics* **79** no. 9, (Aug, 2016) 096001, arXiv:1512.00637 [cond-mat.quant-gas].

[21] H.-P. Breuer and F. Petruccione, *The theory of open quantum systems*. Oxford University Press, Great Clarendon Street, 2002.

Appendix A

Schwinger-Keldysh Path Integral

The Schwinger-Keldysh formalism is an incredibly powerful and widely used tool. Not only does it allow the computation of all Lorentzian correlators without going to Euclidean time (compared to the standard path integral formalism which only allows computation of time-ordered correlators), but it also provides a unified description of unitary and non-unitary theories, equilibrium and non-equilibrium systems, and the evolution of both pure and mixed states.

The key is performing the path integral along a CTP as in Figure A.1, or equivalently doubling the degrees of freedom. The CTP is a curve in complex-time that starts at some initial time t_i, proceeds to some future time t_f, does a small imaginary shift to $t_f - i\epsilon$, and finally returns to $t_i - i\epsilon$. For thermal theories, an additional shift by $-i\beta$ is added to the end, and the two ends of the path are identified. The degrees of freedom $\phi(t_C)$ and operators $O(t_C)$ [1] are defined for any $t_C \in C$ along the path.

We can then obtain a generating functional for a system beginning in state $|\Omega\rangle$ at time t_i:

$$Z_{SK}[J] = \langle\Omega|\mathcal{T}_C \exp\left(\int_C \mathcal{L}[\phi] + J\phi\right)|\Omega\rangle, \tag{A.1}$$

allowing us to define correlation functions of operators similarly to the standard path integral, except operators are ordered based off their position on the path via the contour ordering operator $\mathcal{T}_C$. [2]

[1] We suppress the spatial dependence of ϕ and O

[2] For example, an operator on the reverse leg, at $t_1 - i\epsilon$, always comes after one on the forward leg, at t_2, regardless of the values of t_1 and t_2. Also note that operators solely on the reverse path are

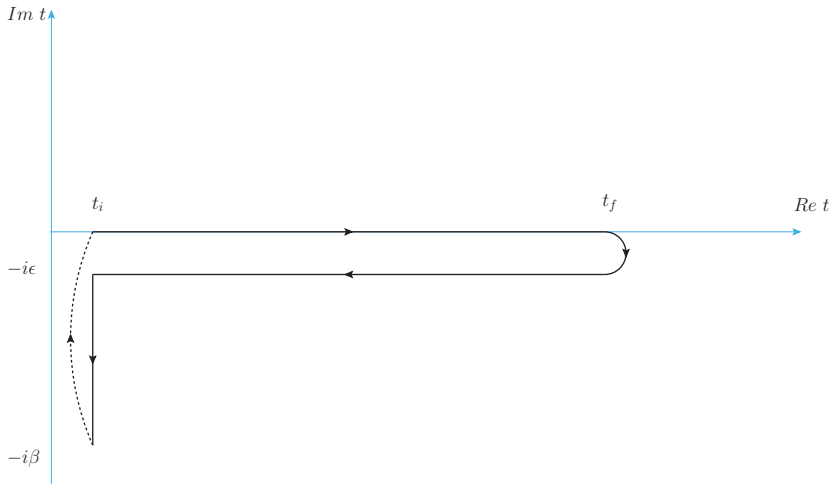

Figure A.1: An example of a closed time path. The dotted line demonstrates that the two ends of the contour are identified with each other.

One can then split the degrees of freedom into one set that lives on the forward leg of the contour, $\phi_1(t)$, and a second that lives on the reverse leg of the contour, $\phi_2(t)$, where $t \in [t_i, t_f]$ is the real, physical time; similarly, operators are defined to live on one path or the other, with separate sources for the forward and reverse paths. These degrees of freedom are subject to the boundary condition $\phi_1(t_f) = \phi_2(t_f)$, enforcing the fact that the degrees of freedom were originally identified with each other.

There are several ways to justify the need for the CTP. One of the most intuitive ways is to consider the standard expectation value of some operator $O(t)$, starting in some state $|\Omega\rangle$ at an initial time t_i:

$$\langle\Omega|O(t)|\Omega\rangle = \langle\Omega|U(t_i,t)O(t_i)U(t,t_i)|\Omega\rangle, \tag{A.2}$$

$$U(t_f,t_i) = e^{-iH(t_f-t_i)}, \tag{A.3}$$

where we have expressed the operator using the Heisenberg equation. This can be interpreted as evolving the state $|\Omega\rangle$ up to the insertion time t with the evolution operator U, inserting the operator $O(t_i)$, and then evolving back to the initial time.

anti-time-ordered, since the path runs backwards in real time.

The justification for the introduction of the standard path integral is to assume our initial state is the ground state of the theory, $|0\rangle$, and that it remains unchanged (up to a phase rotation) under the evolution operator, $U(t_f, t_i)|0\rangle = e^{i\delta}|0\rangle$; then we can write

$$\langle 0|O(t)|0\rangle = e^{i\alpha}\langle 0|U(\infty, t)O(-\infty)U(t, -\infty)|0\rangle. \tag{A.4}$$

Thus we can interpret this as evolving the vacuum from $-\infty$ up to t, inserting the operator $O(-\infty)$, and then continuing the evolution up to $+\infty$. This eliminates the need to "evolve backwards in time", justifying the use of the standard, single contour path integral, with time running from $-\infty$ to $+\infty$.

However, such a procedure isn't justified for generic states. For example, a non-equilibrium state certainly changes upon time-evolution, preventing us from replacing the backwards evolution to the initial time (and hence back to our initial state) with the forward evolution to future infinity. We are forced to keep both the forward and backward evolution operators. We can then say that the degrees of freedom "live" on this single time path that goes forward then backwards, or we can split the degrees of freedom into a set that lives on the forward path and a set on the reverse path, with boundary conditions enforcing equality where the path turns around. The physical operators will always live on the forward path, but it turns out to be more convenient to allow operators to live on both paths, as we will see later.

A more formal way to justify the Schwinger-Keldysh formalism is to consider the evolution of the density matrix of the system from t_i to t_f, i.e.,

$$\rho(t_i) = \sum_j \lambda_j |\Psi_j(t_i)\rangle\langle\Psi_j(t_i)|, \tag{A.5}$$

$$\rho(t_f) = U(t_f, t_i)\rho(t_i)U(t_f, t_i)^\dagger, \tag{A.6}$$

$$Z = \mathrm{Tr}\rho(t_f), \tag{A.7}$$

where we have expressed the density matrix as a generic mixed state, and Z is the partition function corresponding to the evolution of $\rho(t_i)$. Since $U(t_f, t_i)^\dagger = U(t_i, t_f)$, we begin to see (heuristically) that the ket states $|\Psi_j(t_i)\rangle$ are evolved forward in time, while the bra states $\langle\Psi_j(t_i)|$ are evolved backwards in time, corresponding to the doubling of the degrees of freedom where one set evolves backwards in time. The trace operation in Z then forces us to identify the states as equal at t_f,

corresponding to the joining of the forward and reverse legs of the CTP. An excellent source for the details of this interpretation can be found in [20, 21].

The path integral one gets from following this procedure, written in terms of the doubled degrees of freedom (rather than the CTP), is

$$Z_{SK} = \int_{\rho(t_i)}^{\phi_1(t_f)=\phi_2(t_f)} D\phi_1\, D\phi_2\, \exp\left(i\int_{t_i}^{t_f} dt \int d^{d-1}x \mathcal{L}[\phi_1] - \mathcal{L}[\phi_2]\right), \quad \text{(A.8)}$$

where $\phi_{1,2}$ are degrees of freedom defined on the forward and backward contours respectively. The negative in front of $\mathcal{L}[\phi_2]$ is because of the time reversal. The boundary conditions on the functional integral state we are starting in the state defined by $\rho(t_i)$, and that we identify ϕ_1 and ϕ_2 at the time where we reverse the contour.

One of the benefits of the Schwinger-Keldysh formalism is that it allows us to obtain all the standard Lorentzian correlators, rather than just the Feynman correlator. Since operators on the forward contour always come before those on the reverse contour (and since the reverse contour is reverse-time-ordered), we can get four different correlators based on where we insert the operators:

$$\begin{aligned}
G_F(t_1,t_2) &= -i\int_{\rho(t_i)}^{\phi_1(t_f)=\phi_2(t_f)} D\phi_1\, D\phi_2\, \exp\left(i\int d^dx \mathcal{L}[\phi_1] - \mathcal{L}[\phi_2]\right) O_1(t_1)O_1(t_2) \\
&= \langle \mathcal{T} O(t_1)O(t_2)\rangle, \\
G_{\tilde{F}}(t_1,t_2) &= -i\int_{\rho(t_i)}^{\phi_1(t_f)=\phi_2(t_f)} D\phi_1\, D\phi_2\, \exp\left(i\int d^dx \mathcal{L}[\phi_1] - \mathcal{L}[\phi_2]\right) O_2(t_1)O_2(t_2) \\
&= \langle \widetilde{\mathcal{T}} O(t_1)O(t_2)\rangle, \\
G_+(t_1,t_2) &= -i\int_{\rho(t_i)}^{\phi_1(t_f)=\phi_2(t_f)} D\phi_1\, D\phi_2\, \exp\left(i\int d^dx \mathcal{L}[\phi_1] - \mathcal{L}[\phi_2]\right) O_1(t_1)O_2(t_2) \\
&= \langle O(t_1)O(t_2)\rangle, \\
G_-(t_1,t_2) &= -i\int_{\rho(t_i)}^{\phi_1(t_f)=\phi_2(t_f)} D\phi_1\, D\phi_2\, \exp\left(i\int d^dx \mathcal{L}[\phi_1] - \mathcal{L}[\phi_2]\right) O_2(t_1)O_1(t_2) \\
&= \langle O(t_2)O(t_1)\rangle,
\end{aligned} \quad \text{(A.9)}$$

which are the Feynman, anti-Feynman ($\widetilde{\mathcal{T}}$ is the anti time-ordering operator), positive Wightman and negative Wightman correlators. Note that $G_F + G_{\tilde{F}} = G_+ + G_-$. The retarded, advanced, and Keldysh correlators can be obtained from these 4 correlators as well; in fact, upon a changing from the "forward-backward" basis of degrees of freedom to the "average-difference" basis $\phi_r = (\phi_1+\phi_2)/2$, $\phi_a = \phi_1-\phi_2$, one directly obtains these correlators; for example,

$$G_R(t_1, t_2) = i\langle\phi_r(t_1)\phi_a(t_2)\rangle_{SK} = i\Theta(t_1 - t_2)\langle[\phi(t_1), \phi(t_2)]\rangle, \tag{A.10}$$

where $\langle\cdot\rangle_{SK}$ means inserting these operators into the SK action. This is the basis used in Chapter 2 to describe the hydrodynamic effective theory.

Appendix B

Thermal Correlators

We provide a brief review of some of the fundamental results regarding thermal correlators in quantum field theory. We will be working in 0 + 1 dimensions i.e., thermal quantum mechanics; the results can be easily extended to systems with spatial dimensions.

In Minkowski space, there are several types of correlators that appear, including Feynman, retarded, and advanced; determining these propagators in thermal field theories can be a difficult task. Oftentimes, the easiest way is to analytically continue the Lorentzian time to a pure imaginary Euclidean time, $t \to -i\tau$. In this "imaginary time formalism", there is only one well-defined correlator, which can be analytically continued in different ways to obtain all the Lorentzian correlators.

We start with a quantum mechanical system at temperature β with, for simplicity, a discrete energy spectrum. We start by considering the real-time Wightman correlators of position operators; the positive Wightman correlator is

$$\begin{aligned} G_+(t_1,t_2) &= \langle q(t_1)q(t_2)\rangle = \frac{1}{Z(\beta)}\mathrm{Tr}\left[e^{-\beta H}q(t_1)q(t_2)\right] \\ &= \frac{1}{Z(\beta)}\sum_{n,m} e^{-\beta E_n}e^{iE_n(t_1-t_2)}e^{-iE_m(t_1-t_2)}|\langle n|q(0)|m\rangle|^2, \end{aligned} \tag{B.1}$$

where in the second line we inserted a complete basis of energy eigenstates. Since our energy spectrum is bounded from below, we can expect this sum to converge due to the $e^{-\beta E_n}$ factor. (Note that the negative Wightman correlator is just $G_-(t_1,t_2) =$

$G_+(t_2, t_1)$.)

Now let us analytically continue t_1, t_2 to complex values of time. We immediately run into an issue: $e^{-\beta E_n} e^{iE_n(t_1-t_2)} = e^{E_n(-\beta+i(t_1-t_2))}$ and $e^{-iE_m(t_1-t_2)}$ can diverge unless

$$-\beta \leq \mathrm{Im}(t_1 - t_2) \leq 0. \tag{B.2}$$

This leads to the Matsubara correlator, the correlator of position operators at imaginary times τ and 0,

$$G_M(\tau) = G_+(-i\tau, 0) = \langle q(-i\tau)q(0)\rangle = \frac{1}{Z(\beta)}\mathrm{Tr}\left[e^{-\beta H} q(-i\tau)q(0)\right], \tag{B.3}$$

where Equation B.2 demands $\beta \geq \tau \geq 0$. This restriction is why some say the Matsubara correlator is "automatically time-ordered", as it is only guaranteed to exist in time-ordered configurations. Then, the cyclicity of the trace allows one to demonstrate that the function is periodic, $G_M(\tau) = G_M(\tau + \beta)$, thus extending the range of τ.

We can then take the Fourier transform of the Matsubara correlator:

$$G_M(i\omega_n) = \int_0^\beta d\tau e^{i\omega_n \tau} G_M(\tau), \tag{B.4}$$

where $\omega_n = \frac{2\pi}{\beta} n$ are the Matsubara frequencies. Note that $G_M(i\omega_n)$ is defined only on a countable subset of the complex plane.

Finally, demanding that the analytic continuation from the discrete, imaginary Matsubara frequencies to complex z vanish at ∞ and be analytic outside the real axis yields a unique analytic continuation of Equation B.4, $G_M(z)$. This function can be shown to exactly reproduce various real-time correlators. For example, the Fourier transforms of the retarded and advanced correlators are given by

$$\begin{aligned} G_R(\omega) &= G_M(\omega + i\eta), \\ G_A(\omega) &= G_M(\omega - i\eta), \end{aligned} \tag{B.5}$$

i.e., by performing the replacement $i\omega_n \to \omega \pm i\eta$, we obtain the retarded/advanced correlators.

Appendix C

NLO Energy Two-Point Function Details

In this appendix we provide some of the details for the calculation in Section 5.2. The Lagrangian is

$$L = C\Phi^2\left[\ln\frac{1}{\Phi\varepsilon^2} + c\right],\ \Phi \coloneqq \frac{\varphi'(\theta_1)^2\varphi'(\theta_2)^2}{\varphi_{12}^4},\ \varphi_{12} \coloneqq 2\sin\frac{\varphi(\theta_1)-\varphi(\theta_2)}{2}, \quad \text{(C.1)}$$

where $C \coloneqq -\frac{N\gamma\varepsilon^2}{8\pi^2}$ is the constant appearing in Equation 5.1. We are looking for the Noether current associated with simultaneous translation of both times; the fields transform as $\delta\varphi_i = \varphi_i', \varphi_i \coloneqq \varphi(\theta_i)$. The Noether current can then be obtained via $(\partial_1+\partial_2)T_{\text{nl}} \coloneqq \partial_1\left(\delta\varphi_1\frac{\partial L}{\partial\varphi_1'}\right) + \partial_2\left(\delta\varphi_2\frac{\partial L}{\partial\varphi_2'}\right) - \delta L$. We find

$$\delta L = (\partial_1+\partial_2)C\left(\Phi^2\left[\ln\frac{1}{\Phi\varepsilon^2}+c\right]\right), \quad \text{(C.2)}$$

$$\partial_1\left(\delta\varphi_1\frac{\partial L}{\partial\varphi_1'}\right) + \partial_2\left(\delta\varphi_2\frac{\partial L}{\partial\varphi_2'}\right) = (\partial_1+\partial_2)C\left(\Phi^2\left[2\ln\frac{1}{\Phi\varepsilon^2}+2c-1\right]\right), \quad \text{(C.3)}$$

$$\therefore T_{\text{nl}}(\theta_1,\theta_2) = C\left(\Phi^2\left[\ln\frac{1}{\Phi\varepsilon^2}+c-1\right]\right). \quad \text{(C.4)}$$

We now want the generator of $\theta_+ \coloneqq \frac{\theta_1+\theta_2}{2}$ translations, as this is what gives us the energy of the soft mode theory, $E(\tau_+) = \lambda T(\frac{\theta_+}{\lambda})$. Since we are ultimately

interested in the energy two-point function near equilibrium, this means we want Equation C.4 at linear order in $\delta\varphi_i = \varphi_i - \theta_i$:

$$T_{\text{nl}}(\theta_+) = \int d\theta_-\ \theta_{12}^{-4}\left[\left(\delta\varphi_1 + \delta\varphi_2 - \frac{\delta\varphi_1 - \delta\varphi_2}{\tan\frac{\theta_-}{2}}\right)(-4\ln\varepsilon + 2c - 3 + 4\ln\theta_{12})\right]. \tag{C.5}$$

We can now calculate the full energy two-point function at $O(\varepsilon^2)$ as in Equation 5.11. As previously mentioned, the local-local piece was calculated in [17]. We calculate the non-local-local piece by using the leading order soft mode correlator, derived from the Schwarzian action 3.12

$$\langle\delta\varphi_m\delta\varphi_n\rangle^{(-1)} = \frac{1}{2\pi N\alpha_S\varepsilon}\frac{\delta_{m,-n}}{m^2(m^2-1)}. \tag{C.6}$$

We can now calculate the non-local-local piece

$$\begin{aligned}\langle T_{\text{l}}(\theta_+)T_{\text{nl}}(\theta'_+)\rangle^{(-1)} = \sum_{m,n} N\alpha_S\varepsilon\frac{N\gamma\varepsilon^2}{4\pi}\int\frac{d\theta'_-}{2\pi}(-im^3+im)e^{im\theta_+}\theta_{34}^{-4}\,(4\ln\theta_{34} - 4\ln\varepsilon + 2c - 3)\\ \left[(in - \frac{1}{\tan\theta_-/2})e^{in\theta_3} + (in + \frac{1}{\tan\theta_-/2})e^{in\theta_4}\right]\langle\delta\varphi_m\delta\varphi_n\rangle^{(-1)}.\end{aligned} \tag{C.7}$$

By using $\theta_{3,4} = \theta'_+ \pm \frac{1}{2}\theta'_-$, and Equation 5.14, we can solve this integral, giving us Equation 5.13 , restated here for convenience:

$$\langle T_{(\text{l})_m}T_{(\text{nl})_{-m}}\rangle^{(-1)} = -\frac{N\gamma\varepsilon^2}{8\pi^2}\left(-6\ln\varepsilon + 3c - \frac{9}{2} - \frac{8}{3}\partial_h\right)\left(u_{h,\frac{m}{2}} + u_{h,-\frac{m}{2}}\right)\Big|_{h=2}.$$

Finally, since m is an integer,

$$\begin{aligned} u_{h,\frac{m}{2}} + u_{h,-\frac{m}{2}} =& \frac{\Gamma\left(h+\frac{m}{2}\right)}{2\Gamma(2h)\Gamma\left(1-h+\frac{m}{2}\right)} \frac{\cos^2\frac{m\pi}{2}}{\cos\pi h}, \\ \partial_h\left(u_{h,\frac{m}{2}} + u_{h,-\frac{m}{2}}\right) =& \frac{\Gamma\left(h+\frac{m}{2}\right)}{2\Gamma(2h)\Gamma\left(1-h+\frac{m}{2}\right)} \frac{\cos^2\frac{m\pi}{2}}{\cos\pi h} \\ & \left[-2\psi(2h) + \psi\left(1-h+\frac{m}{2}\right) + \psi\left(h+\frac{m}{2}\right) + \pi\tan h\pi\right]. \end{aligned} \tag{C.8}$$

With these formulae, we obtain Equation 5.15.